

**Regulation of mitochondrial RNA editing  
in *Trypanosoma brucei*: The role of RBP7910 in  
parasite life stage transition**

---

**Homa Zamani**

Department of Parasitology

McGill University

Montréal, Canada

November 2024

A thesis submitted to McGill University in partial fulfillment of the requirements  
of the degree of Master of Science

©Homa Zamani, 2024

## Table of contents

<b>1. List of Figures and Tables</b> .....	<b>4</b>
<b>2. List of Abbreviations</b> .....	<b>6</b>
<b>3. Abstract</b> .....	<b>8</b>
<b>4. Acknowledgments</b> .....	<b>12</b>
<b>5. Introduction and Literature Review</b> .....	<b>14</b>
5.1 Trypanosomatid pathogens .....	14
5.2 Life Cycle of <i>Trypanosoma brucei</i> : Adaptations in cell surface proteins and energy metabolism across developmental stages.....	14
5.3 RNA editing in <i>T. brucei</i> : A unique mitochondrial catalytic mechanism essential for survival and adaptation .....	17
5.4 Life-stage specific RNA editing: Molecular components, regulation, and differential functionality .....	20
5.5 Accessory complexes regulating RNA editing .....	24
5.6 The crucial role of RNA binding proteins (RBPs).....	25
5.7 Mitochondrial RNA binding protein 7910 (RBP7910) .....	27
5.8 From a bimodal to a multi-stage view on Trypanosome editing dynamics .....	28
5.9 Importance of Integrating Omics Data .....	29
<b>6. Hypothesis</b> .....	<b>30</b>
<b>7. Objectives</b> .....	<b>31</b>
<b>8. Materials and methods</b> .....	<b>33</b>
8.1 Growing <i>T. brucei</i> monomorphic BF cells .....	33
8.2 Growing <i>T. brucei</i> pleomorphic BF cells .....	33
8.3 BF to PF cell differentiation and optimization .....	34
8.4 <i>T. brucei</i> slender form differentiation to stumpy forms.....	37
8.5 RBP7910 Cloning and transfection into monomorphic BF and PF <i>T. brucei</i> cells .....	37
8.6 Induction of RBP7910 overexpression in monomorphic BF <i>T. brucei</i> .....	38
8.7 Investigation of the potential effects of RBP7910 overexpression on the monomorphic BF life cycle .....	39
8.8 V5 tagged-RBP7910 immunoprecipitation and mass spectrometric analysis .....	41
8.9 Identification of RNA-dependent and -independent interacting protein partners of RBP7910-3V5.....	44
8.10 Omics Data Collection and Analysis .....	46
8.10.1 Proteomic profiling of RNA editing machinery and the classification of RNA-processing complexes .....	46

8.10.2	Translational efficiency analysis in <i>T. brucei</i> .....	47
8.10.3	RNAi Knockdown and Functional Analysis.....	48
8.10.4	Post-translational modifications and the role of RBPs .....	48
8.10.5	Environmental stimulation for <i>in vitro</i> differentiation.....	48
<b>9.</b>	<b>Results</b> .....	<b>50</b>
9.1	Optimization of direct BF to PF cell differentiation in monomorphic and pleomorphic <i>T. brucei</i> .....	50
9.2	Indirect BF to PF cell differentiation in pleomorphic <i>T. brucei</i> .....	52
9.3	Transfected monomorphic BF SM427 cells expressed V5-tagged RBP7910 .....	54
9.4	Overexpression of RBP7910 in monomorphic BF <i>T. brucei</i> induces changes resembling PF differentiation .....	55
9.5	Immunoprecipitation of V5-tagged RBP7910 .....	61
9.6	Mass spectrometry profiling of RBP7910-3V5: Characterization of RNA-mediated and direct protein interactions .....	63
9.7	Editosome protein Abundance profile During SS-to-PF Differentiation .....	66
9.8	Translational Efficiency in <i>T. brucei</i> .....	70
9.9	Role of RNA Binding Proteins .....	70
9.10	Post-translational modifications in Gene Expression Regulation.....	72
9.11	The role of RNA Editing and Environmental Cues in Mitochondrial RNA Processing 72	
<b>10.</b>	<b>Discussion</b> .....	<b>74</b>
<b>11.</b>	<b>Conclusion and summary</b> .....	<b>82</b>
<b>12.</b>	<b>Future directions</b> .....	<b>86</b>
<b>13.</b>	<b>References</b> .....	<b>87</b>
<b>14.</b>	<b>Appendix</b> .....	<b>93</b>

## 1. List of Figures and Tables

<b>Figure numbers</b>	<b>Figure legends</b>
<b>Fig. 1</b>	<i>Cell cycle dynamics in Trypanosoma brucei.</i>
<b>Fig. 2</b>	<i>Mitochondrial DNA structure of Trypanosoma brucei.</i>
<b>Fig. 3</b>	<i>Trypanosoma. brucei RNA editing.</i>
<b>Fig. 4</b>	<i>Regulation of mitochondrial RNA processing in Trypanosoma brucei.</i>
<b>Fig. 5</b>	<i>Stage-specific RNA editing in Trypanosoma brucei mitochondrial mRNAs.</i>
<b>Fig. 6</b>	<i>Stage-specific expression of RBPs in the T. brucei life cycle.</i>
<b>Fig. 7</b>	<i>Morphological changes during direct BF to PF cell differentiation in monomorphic and pleomorphic T. brucei.</i>
<b>Fig. 8</b>	<i>Expression of EP procyclin as a marker of PF differentiation by induced monomorphic and pleomorphic T. brucei.</i>
<b>Fig. 9</b>	<i>Induction of indirect BF to PF cell differentiation in pleomorphic T. brucei cell line.</i>
<b>Fig. 10</b>	<i>Schematic view of RBP7910 overexpression in SM427-plew100-RBP7910-3V5 cell line.</i>
<b>Fig. 11</b>	<i>Tetracycline-induced expression of V5-tagged RBP7910 in monomorphic BF T. brucei SM427 cells.</i>
<b>Fig. 12</b>	<i>Overexpression of RBP7910 in BF cells results in more developed and enlarged mitochondria.</i>
<b>Fig. 13</b>	<i>Experimental setup to assess the impact of RBP7910 overexpression on cell cycle progression in monomorphic BF T. brucei.</i>
<b>Fig. 14</b>	<i>Western blot analysis showing EP procyclin expression in response to RBP7910 overexpression, CCA treatment, and cold shock in BF T. brucei.</i>
<b>Fig. 15</b>	<i>Confirmation of RBP7910 overexpression in the tetracycline-induced cells</i>
<b>Fig. 16</b>	<i>Purification and analysis of V5-tagged RBP7910 interacting partners in the PF (top) and the BF(bottom) T. brucei, with and without RNase treatment.</i>
<b>Fig. 17</b>	<i>Cytoscape PPI network analysis of RBP7910 interacting partners in the PF (top) and the BF (bottom) T. brucei, derived from LC-MS analysis of three eluates.</i>
<b>Fig. 18</b>	<i>Comparative expression profiles of mitochondrial mRNA processing and kinase activity proteins during BF to PF differentiation in T. brucei.</i>

<b>Table number</b>	<b>Table titles</b>
<b>Table 1</b>	<i>Optimization of direct BF to PF differentiation in monomorphic and pleomorphic T. brucei trying various differentiation conditions</i>
<b>Table 2</b>	<i>Designing various experimental conditions for the study of RBP7910 overexpression effects on T. brucei monomorphic BF life stage</i>
<b>Table 3</b>	<i>Results of optimization for the direct BF to PF differentiation in monomorphic and pleomorphic T. brucei</i>
<b>Table 4</b>	<i>Classification of RBP7910 interacting proteins in T. brucei BF identified by LC MS analysis</i>
<b>Table 5</b>	<i>Expression patterns of mitochondrial RNA-processing proteins during SS to PF differentiation in T. brucei</i>

## 2. List of Abbreviations

A/U	Adenine/Uridine
ADAR	Adenosine deaminase acting on RNA
ATP	Adenosine triphosphate
BF	Bloodstream form
C/G	Cytosine/Guanine
CCA	Citrate Cis-Aconitate
CK2A2	Casein Kinase 2 Alpha 2
COII/III	Cytochrome oxidase II/III
CO2	Carbone dioxide
Cyb	Cytochrome b
DNA	Deoxyribonucleic acid
DTT	Dithiothreitol
DRBD6A	Double RNA binding domain protein 6A
EDTA	Ethylendiaminetetraacetic acid
EP	Glu-Pro
ETC	Electron transport chain
FBS	Fetal bovine serum
G418	Geneticin
gDNA	Guide DNA
GO	Gene ontology
GPEET	Gly-Pro-Glu-Glu-Thr
GPI	Glycosylphosphatidylinositol
GRBC	Guide RNA binding complex
h	Hour
hADAR	Human ADAR
HCl	Hydrogen chloride
IP	Immunopercipitation
KCl	potassium chloride
KMRP1/2	Kinetoplast mitochondrial RNA-binding proteins 1/2
KPAC	Kinetoplast polyadenylation complex
KPAF1	Kinetoplast polyadenylation factor 1
KREH	Kinetoplast RNA editing helicase
KREL1/2	Kinetoplastid RNA editing ligase 1/2
KREN 1/2	Kinetoplastid U-deletion endonuclease 1/2
KREPA/B	Kinetoplastid RNA editing protein A/B
KREX 1/2	Kinetoplastid 3'-5' U-specific exonuclease 1/2
LC-MS	Liquid Chromatography coupled with Mass Spectrometry
LS	Long slender
MEAT1	Mitochondrial editing-like complex-associated TUTase 1
MgCl2	magnesium chloride
MMP	Mitochondrial membrane potential
MPsome	Mitochondrial 3' processome
MS	Mass Spectrometry
mtRNA	Mitochondrial RNA
NaH2PO4	monosodium phosphate
Na2HPO4	sodium phosphate dibasic
NEB	New England Biolabs

NEK12.2	Never in mitosis A (NIMA)-related kinase
OE	Overexpression
PAD1	Proteins associated with differentiation 1
PAMC	Polyadenylation mediator complex
PARP	Procyclic acidic repetitive protein
PBS-G/T	Phosphate Buffered Saline with Glucose/Tween
PF	Procyclic form
PPsome	Pyrophosphohydrolase
PTM	Post translational modification
RBP7910	RNA binding protein 7910
rDNA	Ribosomal DNA
RECC	RNA editing catalytic complex
REH2C	RNA editing helicase 2 complex
REMC	RNA editing mediating complex
RESC	RNA editing substrate binding complex
RNA	Ribonucleic acid
RNAi	RNA interference
RRF-Seq	Ribosomal RNA fragment sequencing
SDS-PAGE	Sodium dodecyl-sulfate polyacrylamide gel electrophoresis
SIF	Stumpy induced factor
SILAC	Stable isotope labeling by amino acids in cell culture
SM-427	Single marker 427
SS	Short stumpy
TbRGG2	T. brucei RGG-containing protein 2
TDB	Trypanosome dilution buffer
Tet	Tetracycline
TUTase	Terminal uridyltransferase
UTR	Untranslated region
VSG	Variant surface glycoprotein
WB	Western blot
WT-29.13	Wild type 29.13
ZBD	Z-binding DNA
ZBP	Z binding protein
ZFP3	Zinc Finger Protein 3

### 3. Abstract

Human and livestock parasitic infections caused by trypanosomatid protozoa, such as Sleeping sickness, Nagana cattle disease, Chagas disease, and Leishmaniasis, impose substantial economic and global health burdens, impacting populations across diverse regions, including North America. As one of the most ancient eukaryotes with high evolutionary divergence from well-studied organisms of the domain, *Trypanosoma brucei*, the focus of this study, has a complex life cycle through which it alternates between the two major developmental stages, bloodstream form in the mammalian host and procyclic form in the tsetse fly vector. Given the drastically different nutritional environments each host provides, these transitions require extensive adaptations in metabolism and gene expression. Consequently, *T. brucei* must modulate mitochondrial gene expression, especially through RNA editing, to convert mRNAs into translatable forms necessary for energy production in the insect host.

The essential RNA editing process is particularly intricate, involving inserting or deleting uridine nucleotides into mitochondrial mRNAs guided by RNA templates, thereby enabling the parasite to produce functional respiratory proteins required for survival in the tsetse fly. The editing is orchestrated by an assembly of more than 70 proteins with dynamic interactions that shift as *T. brucei* transitions between life stages. However, the regulatory mechanisms driving these rearrangements remain unknown, underscoring a critical research area for potential therapeutics.

Our study centers on identifying and characterizing these regulatory mechanisms, focusing on an essential mitochondrial RNA-binding protein, RBP7910, that plays a role in RNA processing for specific mitochondrial transcripts and shows differential expression during *T. brucei*

differentiation. Preliminary experiments indicated that overexpressing of RBP7910 in the bloodstream induces EP-procyclin surface protein expression, a hallmark of the insect stage parasite, suggesting RBP7910's influence on life stage transitions. Further, immunoprecipitation of tagged RBP7910, followed by mass spectrometry analysis, revealed interactions with the RNA editing substrate-binding complex, implicating RBP7910 in RNA editing progression.

This study investigates the environmental signals and regulatory pathways influencing mitochondrial RNA processing and stage-specific metabolic shifts in *T. brucei* through an integrative approach utilizing experimental and computational methods. Our findings suggest that RBP7910 acts as a potential master regulator, coordinating RNA editing activities essential for the parasite's adaptation to its hosts. This regulatory role highlights RBP7910 as a promising target for therapeutic interventions to disrupt the parasite's life cycle and, thereby, its transmission.

## Résumé

Les infections parasitaires humaines et animales causées par des protozoaires trypanosomatidés, telles que la maladie du sommeil, la nagana, la maladie de Chagas et la leishmaniose, imposent des charges économiques et sanitaires substantielles à l'échelle mondiale, touchant les populations de diverses régions, y compris en Amérique du Nord. En tant qu'un des eucaryotes les plus anciens avec une divergence évolutive élevée par rapport aux organismes bien étudiés, *Trypanosoma brucei*, sujet de cette étude, possède un cycle de vie complexe alternant entre deux principaux stades de développement : la forme sanguine chez l'hôte mammifère et la forme procyclique dans le vecteur mouche tsé-tsé. Compte tenu des environnements nutritionnels radicalement différents fournis par chaque hôte, ces transitions nécessitent des adaptations métaboliques et des régulations de l'expression génique approfondies. En conséquence, *T. brucei* doit moduler l'expression des gènes mitochondriaux, notamment par l'édition de l'ARN, pour convertir les ARNm en formes traduisibles nécessaires à la production d'énergie chez l'hôte insecte.

Le processus d'édition de l'ARN, essentiel et particulièrement complexe, implique l'insertion ou la suppression de nucléotides d'uridine dans les ARNm mitochondriaux guidée par des ARN templates, permettant ainsi au parasite de produire des protéines respiratoires fonctionnelles nécessaires à sa survie dans la mouche tsé-tsé. Cette édition est orchestrée par un ensemble de plus de 70 protéines dont les interactions dynamiques se modifient lorsque *T. brucei* passe d'un stade de vie à un autre. Cependant, les mécanismes de régulation qui dirigent ces réarrangements restent inconnus, ce qui souligne un domaine de recherche crucial pour de potentielles applications thérapeutiques.

Notre étude se concentre sur l'identification et la caractérisation de ces mécanismes de régulation, en mettant l'accent sur une protéine essentielle de liaison à l'ARN mitochondrial, RBP7910, qui joue un rôle dans le traitement de certains transcrits mitochondriaux et présente une expression différentielle au cours de la différenciation de *T. brucei*. Des expériences préliminaires ont indiqué que la surexpression de RBP7910 dans la forme sanguine induit l'expression de la protéine de surface EP-procycline, caractéristique du stade insecte du parasite, suggérant que RBP7910 influence les transitions de stade de vie. De plus, l'immunoprécipitation de RBP7910 marquée, suivie d'une analyse par spectrométrie de masse, a révélé des interactions avec le complexe de liaison au substrat d'édition de l'ARN, impliquant RBP7910 dans la progression de l'édition de l'ARN.

Grâce à une approche intégrative combinant des méthodes expérimentales et computationnelles, cette étude examine les signaux environnementaux et les voies de régulation influençant le traitement de l'ARN mitochondrial et les changements métaboliques spécifiques aux stades de *T. brucei*. Nos résultats suggèrent que RBP7910 agit comme un régulateur principal potentiel, coordonnant les activités d'édition de l'ARN essentielles pour l'adaptation du parasite à ses hôtes. Ce rôle régulateur met en évidence RBP7910 comme une cible prometteuse pour des interventions thérapeutiques visant à perturber le cycle de vie du parasite et, par conséquent, sa transmission.

## 4. Acknowledgments

I would like to express my deepest gratitude to my supervisor, Dr. Reza Salavati. Throughout my Master's journey, his invaluable knowledge, unwavering patience, and thoughtful guidance have been instrumental in shaping my research. His constant encouragement and motivating presence instilled in me the confidence to delve deeply into complex ideas and challenges, making my research journey both enjoyable and rewarding. I feel incredibly fortunate to have been part of the Salavati lab and to have had Dr. Salavati's mentorship during these pivotal years.

I am sincerely grateful to my committee members, Dr. Sara Zimmer and Dr. Barbara Papadopoulou, for their insightful feedback, constructive suggestions, and support. Their guidance and perspectives have greatly enriched my research and helped me navigate this challenging yet rewarding path.

I am also immensely grateful to Dr. Tamara Sternlieb for her support and friendship throughout my research. Her dedication, generosity, and kindness have been a continual source of inspiration, helping me navigate challenges and approach my work with renewed confidence. Her assistance, especially in performing cell differentiation assays and immunoprecipitation studies, fostered an uplifting sense of camaraderie and contributed significantly to my development as a researcher.

I extend my heartfelt thanks to my current and previous lab members, who have been an essential part of this journey. I particularly appreciate Nisha Ramamurthy's efforts in producing *T. brucei* RBP7910 overexpression monomorphic cell lines and the preliminary work she had done to study the role of RBP7910 in *T. brucei* cell differentiation. I am grateful to Amin Azimi, who generously shared his expertise in mass spectrometry analysis with me. I am also thankful to Linhua Zhung for her guidance in protein purification techniques.

Furthermore, I am indebted to the professors, staff, and friends within the Department of Parasitology, who welcomed and supported me with open arms. Their kindness and encouragement have been invaluable, fostering a sense of community that has greatly enhanced my academic journey.

I would also like to acknowledge the financial support provided by the BMO Scholarship and the DFW from the Faculty of Parasitology. These awards allowed me to focus wholeheartedly on my

research, relieving the burden of financial hardship and enabling me to pursue my studies to their fullest potential.

Lastly, I owe an immeasurable debt to my family, whose love, encouragement, and sacrifices have been the bedrock of my academic pursuits. Their unwavering belief in me has been a constant source of strength and motivation. Without their support and care, I would not have been able to embark on or complete this journey. For everything they have done, I am forever grateful.

## 5. Introduction and Literature Review

### 5.1 *Trypanosomatid pathogens*

*Trypanosoma brucei* spp., *Trypanosoma cruzi*, and *Leishmania* spp. are parasitic protozoa with evolutionary ties but distinct life cycles and insect vectors—tsetse flies, reduviid bugs, and sand flies, respectively. These pathogens cause various diseases in humans and animals, resulting in high morbidity and mortality rates if left untreated. Additionally, transmission through blood transfusions and organ donations raises concerns in developed countries [1-5]. The lack of effective vaccines complicates prevention, and current treatments are limited, often toxic, and ineffective. Increasing drug resistance has further reduced the efficacy of some antiparasitics, underscoring the need for pharmaceutical strategies.

*T. brucei*, the central focus of this study, is an extracellular pathogen that invades the bloodstream, affects the central nervous system, and causes human sleeping sickness and nagana in cattle. Beyond health implications, the disease negatively impacts the economies of 36 sub-Saharan African countries where tsetse flies transmit the infection, affecting both animal health and agriculture [6].

### 5.2 *Life Cycle of Trypanosoma brucei: Adaptations in cell surface proteins and energy metabolism across developmental stages*

The life cycle of *T. brucei*, a vector-transmitted parasite, involves two distinct replicative stages, each occurring in a different host: the mammalian host and the tsetse fly vector. These stages

involve significant changes in gene expression, leading to shifts in metabolism and morphology, especially in cell surface proteins (Fig. 1).

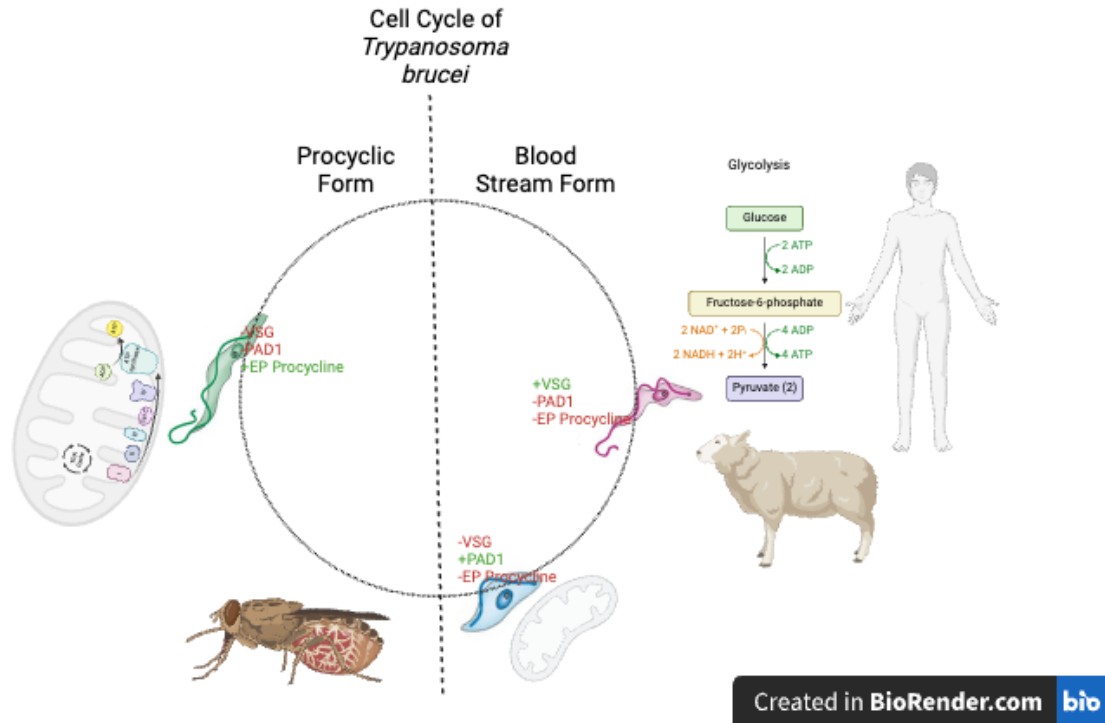


**Fig. 1 Cell cycle dynamics in *Trypanosoma brucei*.** *T. brucei* has a complex life cycle characterized by a transition between two main developmental stages: the bloodstream form, which includes both the proliferative long slender and the non-proliferative short stumpy forms in the mammalian host and the procyclic form in the tsetse fly vector. During these transitions, *T. brucei* undergoes significant changes in surface protein expression to evade the host immune response. In the bloodstream form, the long slender cells express variant surface glycoprotein (VSG), while short stumpy cells are marked by the presence of PAD1 protein. In contrast, the procyclic form in the tsetse fly expresses EP procyclin instead of VSG. To adapt to varying environments and nutrient availability, *T. brucei* also shifts its energy metabolism, moving from a glycolysis-dominant pathway in the bloodstream form to oxidative phosphorylation in the procyclic form. This metabolic adaptation is accompanied by structural changes in the mitochondria, which are larger and contain more developed cristae in the procyclic form, enabling efficient ATP production in the insect vector.

In the mammalian bloodstream, *T. brucei* exists in a slender bloodstream form (slender BF), which transitions into the stumpy bloodstream form (stumpy BF) to prolong parasitemia and prepare for transmission to the tsetse fly. In the fly, the parasite differentiates into the replicating procyclic form (PF) and eventually reaches the infective metacyclic stage, ready for transmission to another mammalian host [7].

Throughout its developmental stages, *T. brucei* undergoes extensive structural and metabolic changes essential for its adaptation to new environments, as demonstrated by both this study and others [8, 9]. The upregulation and downregulation of hundreds of proteins drive these changes, facilitating a switch from mitochondrial respiration in the insect PF to aerobic glycolysis in the mammalian BF. The expression of surface proteins also adapts with each life stage [7].

In the BF, the parasite expresses variant surface glycoproteins (VSGs), which are replaced by procyclin when transitioning to the PF in the insect host. These mutually exclusive surface proteins—VSG in the BF and procyclins in the PF—serve as stage markers. Procyclins, anchored via glycosylphosphatidylinositol (GPI), are of two main types: EP procyclins with 21-27 Glu-Pro repeats (EP1, EP2, EP3, etc.) [10, 11], and GPEET procyclins with five Gly-Pro-Glu-Thr repeats [12-14]. Initially, newly transformed PFs express both GPEET and EP procyclins, but over time, only EP procyclins remain by day 7 in culture [15, 16]. As the parasite prepares for human transmission in the fly's salivary glands, EP procyclins are present during the intermediate epimastigote stage but are suppressed in the final infective metacyclic stage.

In the mammalian host, under optimal conditions, the LS BF can differentiate into the stumpy BF. While the slender BF relies on glucose, the stumpy BF begins adapting to the low-oxygen

conditions expected in the fly's midgut by partially activating mitochondrial functions [17](Fig. 1). These changes in mitochondrial activity and enzyme function enable the parasite to survive in glucose and oxygen-deprived environments [16]. The stumpy BF is non-replicative but remains competent for transmission[18, 19]. The nucleus and mitochondrial DNA (kinetoplast) divide during this stage, but the cells are arrested in the G0/G1 phase and do not survive long-term[20].

Laboratory strains of BF can be either pleomorphic or monomorphic. Pleomorphic strains can transition from slender BF to stumpy BF and complete cell division, whereas monomorphic strains are arrested in the G1/G0 phase and do not survive under differentiation conditions for extended periods. *In vitro* differentiation can be triggered by exposure to citrate cis-aconitate (CCA) and temperature reduction [21]. Understanding the regulatory mechanisms behind these transformations is essential, as they underpin the biology of *T. brucei* and present potential targets for therapeutic intervention. By targeting these differentiation pathways, we may pave the way for novel interventions or preventative measures against trypanosomatid infections.

### ***5.3 RNA editing in T. brucei: A unique mitochondrial catalytic mechanism essential for survival and adaptation***

In *T. brucei*, energy metabolism relies on mitochondrial function, which is critical to the parasite's survival and adaptation across different life stages. A unique feature of *T. brucei*'s mitochondrial biology is RNA editing, a post-transcriptional mechanism that modifies mRNA transcripts by inserting or deleting uridine (U) residues. Guided by small RNAs called guide RNAs (gRNAs) this process generates functional mRNAs required to synthesize components of the electron transport chain (ETC)—a vital pathway for mitochondrial energy production. The complexity and precision of RNA editing in *T. brucei* have attracted considerable research

interest, highlighting a regulatory mechanism specific to kinetoplastids. Understanding RNA editing's intricate role in *T. brucei* could offer potential therapeutic strategies, as disrupting this essential mechanism could impair the parasite's metabolic adaptation and viability in its host.

The kinetoplast, a specialized mitochondrial structure, contains a network of circular DNA molecules categorized into two types: maxicircles and minicircles. Maxicircles encode 18 protein-coding genes and a few gRNAs, while minicircles produce most gRNAs. Six of the maxicircle genes are translated directly, whereas 12 require RNA editing to become translatable [22]. (Fig. 2)

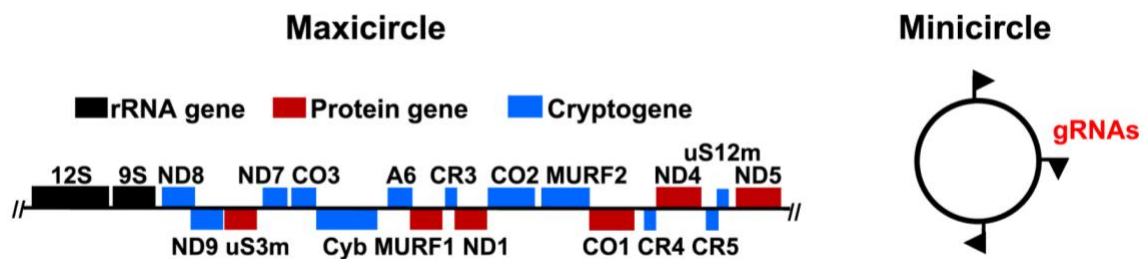


**Fig. 2 Mitochondrial DNA structure of *Trypanosoma brucei*.** *T. brucei* contains two circular sets of mitochondrial DNA, including maxicircles (left) and minicircles (right). While maxicircles encode for 18 mitochondrial protein-coding genes (shown in blue indicating the ones which need editing to produce translatable transcripts and red indicating the never-edited transcripts), two rRNAs (shown in black), and a few gRNAs, minicircles produce most gRNAs [23].

The editing process involves multiple RNA-binding protein complexes, including the RNA editing catalytic complex (RECC), which mediates U-insertion and deletion [17, 24]. The editing begins when the 5' end of a gRNA pairs with a complementary sequence downstream of the first editing site on the precursor mRNA [25]. The gRNA's U-tail further stabilizes the duplex through interactions with purine-rich regions [26, 27]. Mismatches at the editing site are then

recognized by endonucleases (KREN1/2), which cleave the mRNA. Terminal uridylyl transferase 2 (TUTase 2, or KRET2) inserts U residues, while exoribonucleases (KREX1/2) remove U residues as needed. Finally, ligases (KREL1/2) rejoin the mRNA fragments, and RNA editing helicase (KREH) unwinds the mRNA/gRNA duplex, allowing the process to continue with the next gRNA [28-30]. (Fig. 3)

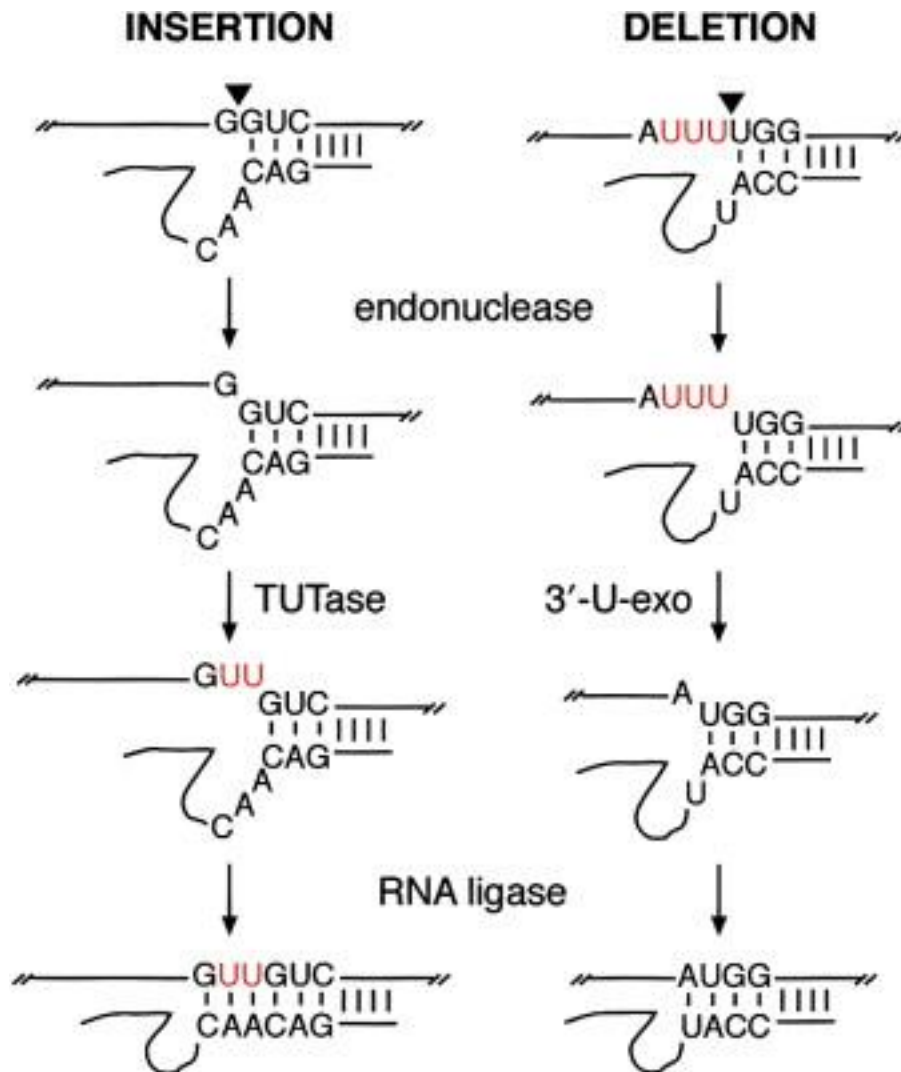


**Fig. 3 Trypanosoma. brucei RNA editing.** The diagram illustrates two distinct RNA editing pathways: insertion editing on the left and deletion editing on the right. In both pathways, pre-mRNAs are paired with gRNAs, which determine the number of uridylyl residues to be added or removed. Arrows indicate

the specific sites of these modifications. During insertion editing, TUTase enzymes add uridylyate residues (shown in red), whereas in deletion editing 3'-U-exonuclease enzymes remove these residues, also highlighted in red. This stepwise editing process is precisely directed by the sequence instructions in the gRNA, ensuring accurate uridylyate modification [31].

#### ***5.4 Life-stage specific RNA editing: Molecular components, regulation, and differential functionality***

RNA editing is regulated differently between the BF and PF stages of *T. brucei*, as shown in Figure 3. In PF cells, all respiratory complexes are required for energy metabolism, whereas oxidative phosphorylation is absent in the BF stage. Typically, complexes I, III, and IV pump protons to generate the mitochondrial membrane potential (MMP) [32]. However, in BF parasites, complex V maintains the MMP by hydrolyzing ATP [33]. This regulation of respiratory complexes is developmentally controlled through RNA editing.

Maintaining MMP is crucial for various cellular functions, such as lipid biogenesis, mitochondrial protein import, and calcium homeostasis [33]. RNA editing is essential in both life stages, as shown by knock-down and knock-out studies[34, 35]. Figure 4 shows the mRNAs that are predominantly edited in PF, those primarily edited in BF, and those edited in both stages.

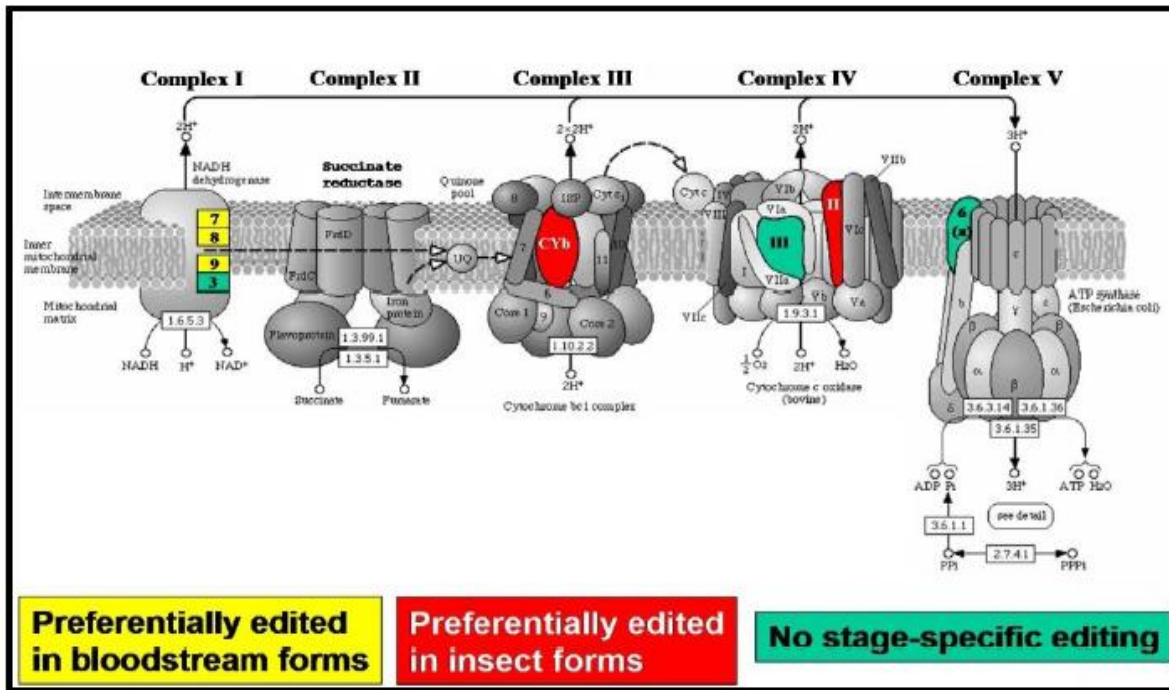


**Fig. 4 Stage-specific RNA editing in *Trypanosoma brucei* mitochondrial mRNAs.** The figure shows mRNAs that undergo predominant editing in the PF (shown in red), BF (shown in yellow), and those that are edited in both stages (shown in green). PF-predominant mRNAs are essential for energy metabolism in the insect vector, while BF-predominant mRNAs support survival in the mammalian host. This stage-specific editing highlights the parasite's ability to regulate mitochondrial gene expression in response to environmental changes throughout its life cycle [36].

The RNA editing machinery in *T. brucei* comprises a complex holoenzyme called the editosome, which includes approximately 45 proteins. This machinery consists of both catalytic and non-catalytic components: the RNA editing catalytic complexes (RECCs) with 21 proteins, the non-catalytic RNA editing substrate-binding complex (RESC) with 21 proteins, and RNA helicase complexes (REH2C) with 3 proteins. Additionally, RNA editing requires coordinated action with over 30 other mitochondrial mRNA processing factors. These include auxiliary factors involved in both 5' processing of primary transcripts by the 5' pyrophosphate processome (PPsome) and 3' trimming by the mitochondrial 3' processome (MPsome). This system also involves A-tailing

and A/U-extensions facilitated by the KPAP1 poly(A) polymerase, polyadenylation factors, and the KRET1 terminal uridylyltransferase (TUTase), all essential for mRNA translation [23].

Current translation models highlight the role of long, heterogeneous 3' mitochondrial RNA tails in ribosome association, with recent evidence showing that mitochondrial RNA (mtRNA) 3' A/U tail addition varies between the two main life stages of *T. brucei* [37]. Interestingly, a proposed model of mRNA circularization suggests that RESC may mediate the association of the 5' PPSome with the 3' end of mitochondrial transcripts, stabilizing mRNA and enhancing its resistance to degradation and uridylation (Fig. 5).

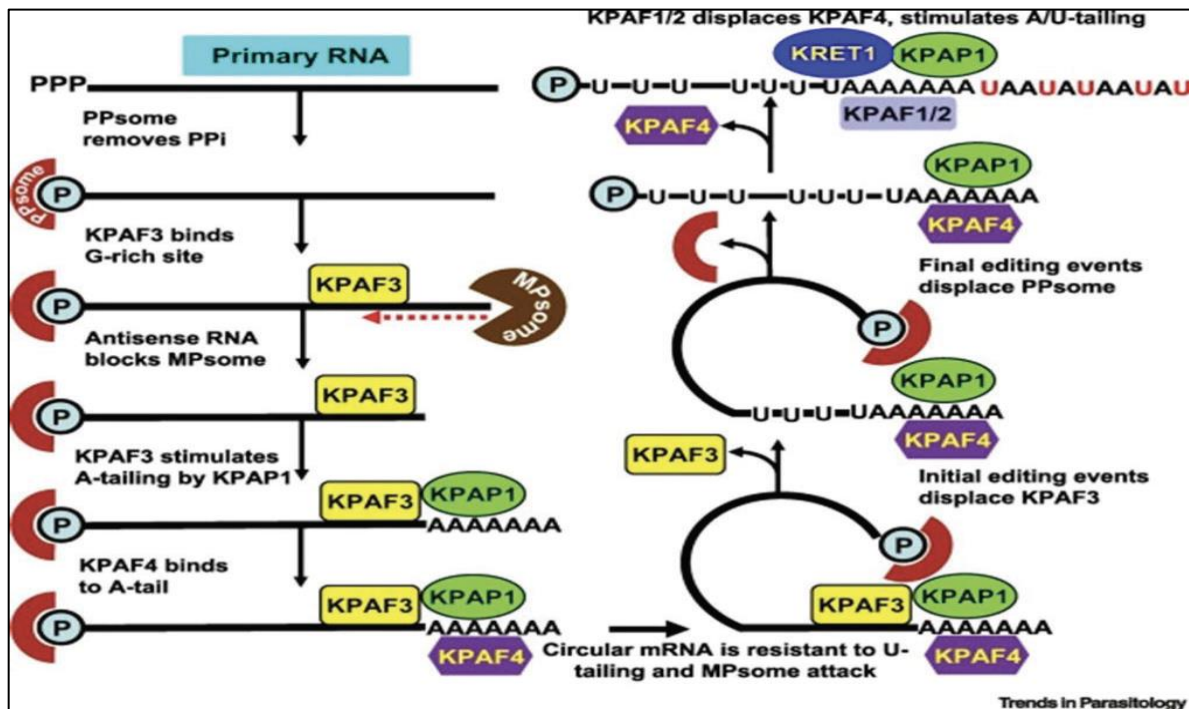


**Fig. 5 Regulation of mitochondrial RNA processing in *Trypanosoma brucei*.** Mitochondrial RNA processing, stability, terminal modifications, and translational activation in *T. brucei* are primarily governed by sequence-specific PPR RNA-binding proteins. Initially, primary mRNA undergoes pyrophosphate (PPI) removal by the PPSome complex, along with 3' end processing by the MPsome

complex. A quality checkpoint likely ensures that the PPsome occupies the 5' end, while 3'–5' trimming terminates correctly downstream of the KPAF3 binding site. In this model, KPAF3 binding appears to select an appropriate 3' UTR from the trimmed isoforms, promoting polyadenylation of the selected precursor by KPAP1. Subsequently, KPAF4 binding to the nascent A-tail may facilitate interaction with the PPsome at the 5' end, enabling mRNA circularization. As a result, only A-tailed mRNAs proceed through the editing cascade, while variants truncated beyond the KPAF3 binding site are targeted for uridylation and degradation. Upon completion of editing at the 5' end, a signaling event likely disrupts circularization, allowing KPAF1/2 factors and KRET1 TUTase access to extend the short A-tail into a long A/U-tail. While these hypotheses require further validation, it is plausible that final editing events displace the PPsome from the 5' end, serving as the signaling event for mRNA maturation, particularly in the case of pan-edited mRNAs. *Abbreviations:* PPP: 5'-triphosphate group; PPi: inorganic pyrophosphate; PPsome: 5' pyrophosphate processome; MPsome: mitochondrial 3' processome [23].

One subcomplex of RESC, RESC19 (also known as RBP7910), has been implicated in this circularization, potentially increasing mRNA stability by delaying A/U-tailing and promoting the translation activation of partially processed transcripts [23].

While editosome proteins are conserved mainly between the BF and insect PF stages, evidence from mutational studies suggests they may function differently across these stages, contributing to stage-specific RNA editing. For example, identical mutations in the non-catalytic RECC proteins KREPA3 and KREP5—essential for survival in both BF and PF stages, where they support viability, RNA editing, and editosome structure—show distinct effects on growth, editing, and editosome integrity between these stages [38, 39]. This stage-specific impact aligns with the differential presence of edited mitochondrial transcripts in the ETC across BF and PF stages.

Although the temperature difference (around 10°C) between BF and PF stages can influence mRNA structure and gRNA utilization, differential RNA editing is not due to gRNA abundance [40, 41]. Instead, the differential utilization of gRNAs by editosome proteins during stage transitions may drive these editing differences [40-44]. This raises important questions about the mechanisms regulating gRNA association with the editing machinery across life stages: Is temperature the primary signal influencing differential editing, or do other environmental cues modulate editosome functionality? What regulatory factors mediate the stage-specific functions of editosome components during differentiation?

### ***5.5 Accessory complexes regulating RNA editing***

Accessory complexes play a critical regulatory role in RNA editing, complementing the catalytic functions of RECC in uridine insertion/deletion. Several protein complexes, such as the guide RNA binding complex (GRBC), also known as mitochondrial RNA binding complex 1 (MRB-1), are essential for *in vivo* editing [45-47]. Proteins GRBC1 and GRBC2 help stabilize gRNAs and link the GRBC complex to RNA editing [46, 48]. As knockdown studies show, RNA editing initiates within the GRBC complex [22, 44, 49]. GRBC also interacts with the polyadenylation mediator complex (PAMC) and the RNA editing mediator complex (REMC), which contains TbRGG2, an RNA binding protein involved in RNA editing progression and gRNA utilization. Together, GRBC, REMC, and PAMC form the RNA editing substrate-binding complex (RESC), which partners with RECC to create the complete editosome holoenzyme [24]. Additionally, mitochondrial RNA binding proteins MRP1 and MRP2 assist in gRNA-mRNA annealing and stabilization, while RGG1 and RBP38 are thought to contribute to RNA stability [46, 50-52].

### ***5.6 The crucial role of RNA binding proteins (RBPs)***

Gene expression can be regulated at multiple levels, but post-transcriptional control plays a particularly critical role in trypanosomatids [53]. These early-branching eukaryotes have unique mechanisms for gene regulation. Unlike many organisms, *T. brucei* does not regulate gene expression at the level of individual genes through RNA polymerase II transcription initiation. Instead, it uses polycistronic transcription, where multiple genes are transcribed together. Mature mRNAs are then generated via co-transcriptional trans-splicing and polyadenylation, with gene expression relying almost entirely on post-transcriptional regulation [54]. In this system, the interaction between RBPs and mRNAs is central to controlling mRNA maturation, localization, stability, and translation rates [55, 56]. As a result, trypanosomatids serve as valuable models for studying post-transcriptional gene regulation, with recent research identifying mRNA processing as a potential therapeutic target for these parasites [57, 58].

Many RBPs characterized in *T. brucei* are cytosolic and regulate specific mRNAs in a life-stage-dependent manner, influencing parasite differentiation [59]. (Fig. 6)

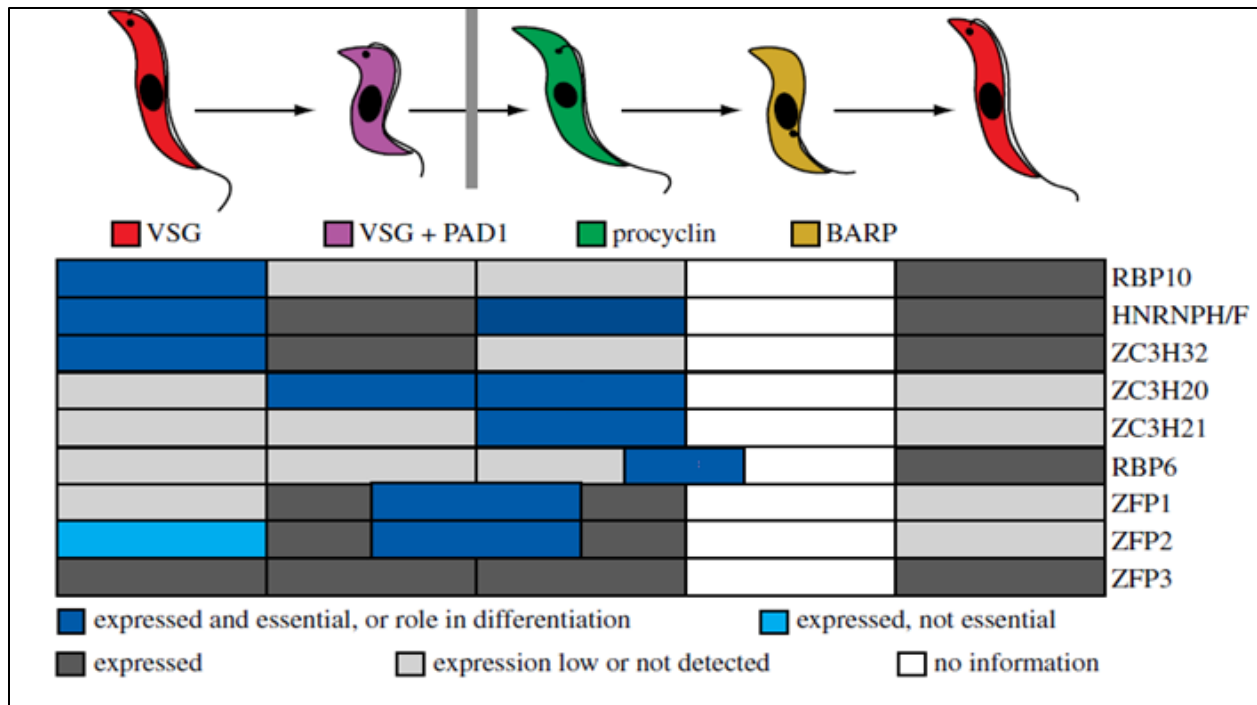


**Fig. 6 Stage-specific expression of RBPs in the *T. brucei* life cycle.** The figure outlines the differential expression of key RBPs across distinct *T. brucei* life stages: BF parasites on the left, shown in red and purple, and PF parasites on the right, shown in green, yellow, and red. The table uses colour coding to indicate each RBP's (including RBP10, RBP6, etc.) role in life stage transitions: dark blue signifies RBP expression and essentiality for *T. brucei* growth and/or differentiation at specific stages; light blue indicates expression without essentiality; dark gray represents expression; light gray shows low expression levels, while white indicates no available information regarding the RBP's role at that stage [60].

For instance, RBP10 is exclusively expressed in BFs; its overexpression (OE) blocks the transition from BFs to PFs, while its depletion leads to increased expression of mRNAs associated with early differentiation stages [61]. The role of RBPs in developmental regulation is further demonstrated by the OE of RBP6, which, in cultured non-infectious PFs, stimulates differentiation into metacyclic forms expressing VSGs, restoring their infectivity to mammals [62]. Thus, RBP6 is pivotal in regulating life-stage-specific gene expression and parasite

differentiation. Additionally, recent studies have identified 22 genes that either promote or inhibit the progressive development toward infectivity at various stages [63].

### ***5.7 Mitochondrial RNA binding protein 7910 (RBP7910)***

Using innovative experimental and computational approaches, coupled with a systematic analysis of protein complexes in *T. brucei*, we identified novel factors associated with mtRNA processing in the parasite. Independent experiments further validated these findings [64]. Genetic studies revealed that the protein encoded by Tb927.10.7910 influences RNA editing and the stability of certain mitochondrial proteins, although its precise role remained unclear. This protein, now designated RNA-binding protein 7910 (RBP7910), contains Z-DNA binding domains (ZBDs) and binds with high specificity and affinity to target mRNAs with A/U-rich sequences and with a notable affinity for (CG)<sub>n</sub> Z-DNA [65, 66]. ZBDs are found in other Z-DNA binding proteins (ZBPs), such as human adenosine deaminase acting on RNA (hADAR) [65]. These domains recognize and stabilize the Z-form of DNA or RNA, which adopts a left-handed conformation. The Z-conformation of nucleic acids is typically induced by enzymes that unwind double-stranded RNA or DNA, particularly in purine-pyrimidine-rich sequences like (CG)<sub>n</sub> or (AU)<sub>n</sub> [67].

Further investigation revealed that RBP7910 interacts with other mitochondrial RNA processing enzymes in an RNA-dependent manner [64]. This interaction was independently corroborated by another study that identified RBP7910 through pull-down experiments as part of the PPsome complex, involved in the processing of purine-rich edited transcripts [68].

### ***5.8 From a bimodal to a multi-stage view on Trypanosome editing dynamics***

Historically, the study of RNA editing in *T. brucei* has predominantly followed a bimodal model, focusing on the distinct life stages of BF and PF parasites [49, 69]. While this model has provided valuable insights into the differential regulation of mitochondrial RNA editing during these transitions, emerging evidence suggests that a more nuanced, multi-stage view is essential to fully understand RNA editing dynamics in trypanosomes. Research now highlights the dynamic regulation of RNA editing across multiple life stages, supporting a shift from a bimodal to a multi-stage model. [70].

Recent findings indicate that RNA editing is not a simple binary switch between states but rather a complex, stage-dependent process characterized by a continuum of regulatory events. This multi-stage perspective encompasses various intermediate states and the influence of environmental factors, providing a deeper understanding of how *T. brucei* adapts its RNA editing machinery in response to different physiological contexts [71].

Notably, studies have demonstrated that editing machinery is modulated at the differentiation endpoints and during intermediate stages. Factors such as cold shock and nutrient availability have been shown to influence RNA editing patterns, indicating a regulatory framework that extends beyond the BF-to-PF switch alone [72].

This evolving perspective reveals that RNA editing in trypanosomes is subject to a range of regulatory influences, including post-transcriptional modifications [73] and interactions with RBPs [74]. The integration of high-throughput omics data further supports this multi-stage view,

allowing researchers to investigate the temporal dynamics of RNA editing across various life stages and environmental conditions [70].

Recognizing RNA editing as a multi-faceted process highlights the need for a comprehensive study of its regulation in *T. brucei*. By examining the interplay between various regulatory factors and environmental cues, researchers can uncover the intricate mechanisms that govern RNA editing and ultimately contribute to the parasite's survival and pathogenicity.

### ***5.9 Importance of Integrating Omics Data***

The shift towards a multi-stage view of RNA editing necessitates the incorporation of diverse omics datasets, including transcriptomics and proteomics. These datasets provide valuable insights into the abundance and regulation of both RNA and proteins involved in the editosome function. Recent studies have employed transcriptomic analyses to reveal alterations in mRNA levels during differentiation, while proteomic investigations have quantified protein dynamics across life stages [71, 75].

By leveraging this wealth of omics data, researchers can identify potential candidate regulators of RNA editing and gain insights into the temporal expression patterns associated with various editing processes. Additionally, gene set analyses can further elucidate the functional relationships among key proteins and their roles in regulating editosome activity [70].

## 6. Hypothesis

RBP7910 is a key regulator of mitochondrial RNA editing in *T. brucei*, driving essential differentiation processes and life cycle progression. With a predicted Z-DNA binding motif, RBP7910 is associated with life-stage-specific transcripts, such as Cytochrome b (CYB), indicating its role in controlling differential RNA editing. This study hypothesizes that RBP7910 accomplishes this regulatory function by modulating RNA processing dynamics during the critical transition from the BF to the PF, partly through interactions with mitochondrial multiprotein complexes. These interactions are expected to ensure the proper editing of mRNAs needed for the parasite's adaptation across its life stages.

The primary hypothesis is that RBP7910's influence on mitochondrial RNA processing is both temporally and spatially regulated, affecting BF-to-PF differentiation by enabling stage-specific expression patterns through RNA-dependent and RNA-independent interactions. These interactions are likely facilitated by mitochondrial RNA editing complexes, which ensure accurate mRNA processing for the parasite's metabolic adaptation in each life stage.

Furthermore, it is hypothesized that environmental signals modulate RBP7910's interactions with RNA-editing and mitochondrial RNA-processing complexes, shaping stage-specific responses essential for *T. brucei*'s adaptation. Through these regulatory pathways, RBP7910 ensures that the mitochondrial transcripts necessary for each life stage are properly edited, supporting the survival and proliferation of *T. brucei* across diverse environments.

## 7. Objectives

The primary aim of this project was to characterize the mitochondrial RNA processing dynamics of RBP7910 during the differentiation of *T. brucei*. Specifically, the study assessed how RBP7910 expression influences differentiation pathways between BF and PF stages at various times. Focusing on the monomorphic strain Lister 427 (SM427), the study enabled a detailed understanding of the temporal dynamics involved in this differentiation process.

A second objective was distinguishing between RNA-dependent and RNA-independent protein-protein interactions of RBP7910 during BF to PF differentiation. By examining these interactions in the two BF and PF life stages, the research aimed to provide insights into the molecular mechanisms underlying RBP7910's role in cellular regulation and differentiation.

Building on these findings, a third objective was to investigate the adaptive mechanisms governing mitochondrial RNA processing across different life stages, with a focus on the regulatory protein interactions and environmental signals that shape stage-specific responses. This objective sought to broaden our understanding of how RNA-editing and mitochondrial RNA-processing complexes, including RBP7910, contribute to *T. brucei* differentiation, particularly during the critical BF to PF transition. By linking RBP7910's RNA-dependent and RNA-independent interactions with the broader regulatory environment in the BF and PF parasite, this study aimed to reveal how mitochondrial processing dynamics are modulated across life stages.

Together, these objectives provide a comprehensive understanding of how RBP7910 and its interactions with RNA and protein complexes regulate mitochondrial RNA processing and drive *T. brucei* differentiation. This research highlights the adaptive mechanisms that enable stage-specific responses crucial for the parasite's life cycle transition from BF to PF.

## 8. Materials and methods

### 8.1 Growing *T. brucei* monomorphic BF cells

To grow *T. brucei brucei* monomorphic BF strain (Lister Single Marker (SM) 427) *in vitro*, frozen cells were first thawed from liquid nitrogen using a 37°C water bath and washed twice with 10 mL of HMI-9 medium pre-warmed to 37°C. The cells were then resuspended in 10 mL of the same medium supplemented with 10% (v/v) heat-inactivated fetal bovine serum (FBS) and incubated at 37°C with 5% CO<sub>2</sub>. After six hours, 1 µg/ml G418 was added to maintain the SM cells. Daily checks were performed to monitor growth, considering approximately six hours of doubling time. The monomorphic cells were diluted to approximately  $5 \times 10^4$  cells/mL using a 1:20 dilution whenever the cell density reached  $2 \times 10^6$  cells/mL. The cells were spun down for long-term storage when reaching about  $1 \times 10^6$  cells/mL, resuspended in a freezing solution of 20% glycerol and 60% FBS, and frozen in 1 mL aliquots. These aliquots were placed on ice for one hour, then stored at -70°C for 2–3 days before transferring to liquid nitrogen for permanent storage.

### 8.2 Growing *T. brucei* pleomorphic BF cells

To grow *T. brucei brucei* pleomorphic strain EATRO 1125 BF cells (Anatat1.1 strain; pHD1313 cell line) *in vitro*, frozen cells were first thawed at 37°C water bath and washed twice with 10 mL of pre-warmed regular HMI-9 medium. The cells were cultured in HMI-9 medium supplemented with 10% FBS and 1.1% (w/v) methylcellulose (Methocel A4M, Sigma 94378, Munich, Germany) at 37°C and 5% CO<sub>2</sub> (referred to as HMI9-MC medium). After six hours, 0.2 µg/ml phleomycin was added to maintain the cells. Temperature stability and careful handling

were essential when working with pleomorphic BF cells. Cell counts were conducted regularly using a Neubauer chamber, and population density was maintained below  $5 \times 10^5$  cells/ml to avoid *in vitro* differentiation into the stumpy stage. For routine cultivation, cultures were diluted to the desired cell concentration with pre-warmed HMI9-MC medium containing 0.2  $\mu\text{g/ml}$  phleomycin.

To harvest cells, methylcellulose was removed by diluting the culture 1:4 with pre-warmed trypanosome dilution buffer (TDB) and filtering based on volume. For 10 ml cultures, a sterile pleated filter (MN 615  $\frac{1}{4}$   $\emptyset$  185 mm, Macherey-Nagel, DE) pre-wetted with TDB, was used, and the filtrate was collected in a 50 ml centrifuge tube. For larger volumes, a sterile bottle-top filter unit with a circular filter (MN 615  $\emptyset$  50 mm, Macherey-Nagel, DE). Following filtration, cells were pelleted by centrifugation at 1400g for 15 minutes at 37°C, and the supernatant was discarded.

Growth curves were determined by measuring cell concentration and resuspending them in a fresh culture flask at  $2 \times 10^4$  cells/ml every 24 hours for six days. Population doubling times were calculated using standard formulas.

### ***8.3 BF to PF cell differentiation and optimization***

Several factors were carefully controlled and optimized to successfully induce BF to PF differentiation, including initial cell density, temperature, differentiation medium composition, the addition of metabolites such as CCA, and glucose availability. Each of these variables plays a critical role in determining the efficiency and success of the differentiation process. An experiment was designed to test various combinations of differentiation conditions and optimize

a BF to PF differentiation protocol suitable for both monomorphic (SM427) and pleomorphic cells (pHD1313).

The factors considered were as follows:

**1. Initial cell density:** The initial number of cells can significantly impact differentiation.

Testing different densities ensures optimal growth and development conditions.

**2. Temperature:** A shift from 37°C to 27°C (or cold shock) is a major inducer of BF to PF differentiation.

**3. Composition of PF differentiation induction medium:** The BF to PF differentiation medium must ensure cell survival and support differentiation. Testing various formulations, including HMI-9 and SDM79, helps induce life stage transitions.

**4. Citrate and cis-aconitate (CCA):** These metabolites are crucial for inducing differentiation.

The experiment explored varying concentrations to determine the optimal dose for efficient BF to PF transformation.

**5. Glucose availability:** Glucose levels influence metabolic pathways involved in differentiation. Testing glucose-depleted and glucose-containing PF differentiation environments using SDM79 or SDM80 medium, respectively, helps fine-tune metabolic conditions for successful differentiation.

The table below summarizes the different variables tested in this experiment. The results will inform the final BF to PF differentiation protocol, tailored to both cell types.

**Table 1 Optimization of direct BF to PF differentiation in monomorphic and pleomorphic *T. brucei* trying various differentiation conditions**

Condition no.	Initial cell density (M cells/ml)		Differentiation medium*			Growth medium**			Cis-aconitate Conc. (μM)		Citrate Conc. (μM)		Time of medium exchange (h)	
	1	2	HMI-9	SDM-79	SDM-80	HMI-9	SDM-79	SDM-80	3	6	0	3	0	24
1		■		■			■			■	■		■	
2	■			■			■			■	■		■	
3	■				■			■		■	■			
4	■			■				■		■	■		■	
5	■				■		■							
6	■		■				■			■	■		■	
7	■		■				■							■
8		■	■				■			■	■			■
9	■		■					■		■	■			■
10	■			■			■			■	■			■
11	■			■				■		■	■			■
12	■				■			■		■	■			■
13	■				■		■		■		■			■
14	■		■				■			■		■		■
15	■		■				■		■			■		■
16		■	■				■			■		■		■

\* Initial medium for differentiation induction (0-hour): Specifies the medium used to initiate differentiation, including HMI-9, SDM-79, or SDM-80.

\*\* Medium for culturing induced cells (24-hour): Indicates the medium used for the continued growth of cells after 24 hours, including HMI-9, SDM-79, or SDM-80.

The black colour indicates the selected factor for each specific variable.

Abbreviations: M: million cells, Conc: concentration; h: hour

The indirect differentiation of BF *T. brucei* into PF cells through the SS stage was also established for pleomorphic pHD1313 cells. This method ensures more synchronized differentiation, as all cells reach the same cell cycle stage at the SS form.

To achieve this, pHD1313 BF cells in the LS form were first differentiated into the SS form by following the previously described protocol. Briefly, pHD1313 cells with an initial density of  $5 \times 10^5$  cells/mL were cultured in HMI9 medium supplemented with 1.1% methylcellulose for 48

hours. The medium was then replaced with SDM79 containing 6 mM cis-aconitic acid, and the culture was incubated at 27°C without CO<sub>2</sub> to induce differentiation into PF. After 24 hours, the medium was replaced with fresh SDM79 lacking cis-aconitic acid, and the cells were incubated for an additional 48 hours to allow further morphological changes toward the PF stage. Cells were counted with a Neubauer chamber, and the population density during routine cultivation was maintained between 5x10<sup>5</sup> and 1x10<sup>7</sup> cells/mL. The cultures were diluted to the desired cell density using complete SDM79 with 0.2 µM phleomycin.

#### ***8.4 T. brucei slender form differentiation to stumpy forms***

LS forms of pleomorphic *T. brucei* were differentiated into short stumpy (SS) forms in HMI9 medium supplemented with 1.1% methylcellulose solution. LS forms were grown to a population density of 5 x 10<sup>5</sup> cells/mL and incubated at 37°C and 5% CO<sub>2</sub> for 48 hours to allow stumpy induction factor (SIF) accumulation. Cells were visually assessed for stumpy morphology and for a medium colour change from red to orange. Cells were then harvested via filtration and centrifugation, as described in section 8.2. Proteins associated with differentiation 1 (PAD1) expression as the stumpy-specific protein marker was also checked using the western blot (WB) analysis with an anti-PAD1 antibody (a gift from K. Matthews, University of Edinburgh).

#### ***8.5 RBP7910 Cloning and transfection into monomorphic BF and PF T. brucei cells***

The RBP7910 cloning and transfection into BF and PF *T. brucei* had been previously performed in the lab [76]. Briefly, The RBP7910 gene was cloned into the tetracycline-regulatable pLew100-3v5 plasmid with a phleomycin resistance marker, using HindIII and BamHI sites for insertion. For transfection, the plasmid was linearized with NotI and precipitated. Late-log phase

PF and mid-log phase BF *T. brucei* cells were then prepared in Cytomix solution and electroporated with the linearized plasmid. Transfected cells were cultured in selective media (SDM-79 for PF, HMI-9 for BF) with 15 µg/mL G418 and 50 µg/mL hygromycin for the PF cells and 1.2 µg/mL G418 for BF the cells.

The pLew100-RBP7910-3v5 plasmid includes a phleomycin resistance gene for selecting positive transfectants. Therefore, after 24 hours of incubation of the BF and PF cells at 37°C and 27°C, respectively, phleomycin was added to the culture flasks at a final concentration of 2.5 µg/mL. The culture was then serially diluted in 24-well plates using HMI-9 medium, for also containing 2.5 µg/mL phleomycin, to isolate clonal transfectants. While cells in the control flask did not survive beyond 4-5 days of phleomycin treatment, visible growth began in the serially diluted transfected cultures after about one week of treatment. The positive transfectants from the 24-well plates were transferred to 25 cm<sup>2</sup> culture flasks and monitored for growth over the next week, with an expected doubling time of approximately 6 hours for the BF and 16 hours for the PF cells, respectively.

### ***8.6 Induction of RBP7910 overexpression in monomorphic BF T. brucei***

As previously described, the RBP7910-3v5 gene was integrated into the rDNA spacer region, or "silent region," of the *Trypanosoma brucei* genome, which includes the 18S rRNA and is unaffected by genome read-through transcription. Controlled by a tetracycline-inducible PARP promoter, RBP7910-3v5 is expressed as an ectopic copy, potentially alongside the endogenous version, while the phleomycin resistance gene is driven by a T7 promoter. Monomorphic BF SM427 cells transfected with the pLew100-3v5 plasmid allow for RBP7910-3v5 overexpression (+Tet), with untreated cells (-Tet) serving as controls, showing no ectopic expression [76].

Transfected cells were cultured in a complete HMI-9 medium containing 1 µg/mL G418 and 2.5 µg/mL phleomycin at 37°C with 5% CO<sub>2</sub>. To maintain the cells in the log phase, the cell density was kept between 2 x 10<sup>5</sup> and 2 x 10<sup>6</sup> cells/mL. Tetracycline was added when the cells were in the mid-log phase (~5 x 10<sup>5</sup> cells/mL). Various tetracycline concentrations (0.1, 0.5, and 1 µg/mL) were tested to identify the optimal concentration for RBP7910 OE.

Post-tetracycline addition, cells were incubated at 37°C with 5% CO<sub>2</sub> and harvested at 0, 6-, 12-, 24-, and 48-hours post-induction. Harvesting was performed by centrifugation at 1,400 g for 10 minutes, and the samples were subjected to downstream analyses, including morphological studies and western blotting (WB), to detect V5-tagged RBP7910 expression. Non-induced cells (-Tet) served as a negative control to assess any background expression of the gene of interest.

### ***8.7 Investigation of the potential effects of RBP7910 overexpression on the monomorphic BF life cycle***

A series of conditions were designed to examine the potential regulatory effects of RBP7910 OE on monomorphic BF SM427 cells, with and without cold shock and CCA treatments.

As described in the previous section, to induce RBP7910 OE in monomorphic SM427 cells, 0.5 µg/mL tetracycline was added during the mid-log phase (~5 x 10<sup>5</sup> cells/mL). The cells were cultured in a complete HMI-9 medium supplemented with 1 µg/mL G418 and 2.5 µg/mL phleomycin at 37°C with 5% CO<sub>2</sub>. Post-induction, the cells were incubated under the same conditions and harvested at 0, 6, 12, 24, and 48 hours (Condition 2; C2).

To explore whether an additional factor, such as cold shock, might synergize with RBP7910 OE to induce cell progression, the cells in one condition (C3) were treated with tetracycline and incubated at 27°C instead of 37°C. Additionally, the effects of CCA alone and combined with

cold shock were evaluated (Conditions C4 and C5, respectively) to assess synergistic or inhibitory interactions. Control conditions were established to rule out any confounding regulatory effects of the medium (C6), cold shock (C7), and/or CCA (C8) alone. A positive control (C1) for cell differentiation was also set up using the standard BF to PF differentiation protocol, which includes cold shock and CCA treatment. In total, eight experimental conditions were tested.

**Table 2 Designing various experimental conditions for the study of RBP7910 overexpression effects on *T. brucei* monomorphic BF life stage**

Condition no.	Tet	Cold-shock	CCA
C1			
C2			
C3			
C4			
C5			
C6			
C7			
C8			

The black colour indicates the addition of specific factors in each cellular condition.  
*Abbreviations:* C: condition, Tet: tetracycline, CCA: citrate cis-aconitate

The cells in all eight conditions were harvested at 0, 6, 12, 24, and 48-hour time points through centrifugation at 1300g, 10 minutes, at 4°C, followed by two washes with cold phosphate-buffered saline (PBS) supplemented with 6mM glucose (PBS-G buffer). Approximately 50 x 10<sup>6</sup> cells were lysed each time to extract the protein using 50 µl of protein lysis buffer, which included 10 mM Tris-HCl (pH 7.2), 10 mM MgCl<sub>2</sub>, 100 mM KCl, 1 µg/mL pepstatin, 1 mM DTT, 1% Triton X-100, and 1X EDTA-free protease inhibitor cocktail (Roche), and gently

rotated for 15 minutes at 4°C. The resulting lysate was then treated with 4 units of RNase-free DNase I (Roche) for 1 hour on ice, followed by centrifugation at 16,000 g for 15 minutes at 4°C to clear the solution. The lysates were then snap-frozen in liquid nitrogen and stored at -80°C.

To investigate whether tetracycline-induced (+Tet) cells (C2, C3, C4, and C5) expressed v5 tag and whether non-induced (-Tet) cells did not, as well as to determine if any of the conditions (C1–C8) displayed signs of differentiation toward the PF, WB analysis was performed. The expression of the V5 tag and EP procyclin, a specific marker of PF cells, was examined.

Additionally, the expression of the RBP7910 protein was assessed across various stages of the BF, PF, and at 0, 6, 12, 24, and 48 hours post-induction.

For the WB analysis, protein extracts were mixed with 6X loading buffer and heated at 95°C for 5 minutes. After separation by SDS-PAGE, the proteins were transferred onto membranes and were incubated overnight at 4°C with the following antibodies diluted in 5% skim milk in PBS-Tween 20 (PBS-T) buffer: 1:1000 mouse anti-EP procyclin (Cedarlane) and 1: 2500 mouse anti-V5 TAG (Bio-Rad) antibodies. The membranes were then washed five times with PBS-T and incubated for 1 hour at room temperature with the (secondary antibody: 1:10,000 goat anti-mouse HRP-conjugate (Bio-Rad). Following another five washes with PBS-T, protein detection was carried out using 1:1 mixture of Clarity Western Peroxide and Clarity Western Luminol/Enhancer reagents (Bio-Rad).

### ***8.8 V5 tagged-RBP7910 immunoprecipitation and mass spectrometric analysis***

RBP-7910-3v5 Immunoprecipitation (IP) was performed using Dynabead protein G (Invitrogen), which are uniform, 2.8-µm superparamagnetic beads with recombinant Protein G (~17 kDa),

coupled with anti-V5 tag antibody, and RNase A to identify the RNA-dependent and -independent interacting protein partners of RBP7910 in BF and PF *T. brucei*. Therefore, three experimental setups were used: without tetracycline induction (-Tet; no RBP7910-3V5 expression), with tetracycline induction (+Tet; induced RBP7910-3V5 expression), and with tetracycline and RNase A treatment during precipitation (+Tet+RNase), which removes proteins indirectly bound to RBP7910-3V5 via RNA, leaving only those directly bound to it.

To couple the beads with V5 monoclonal antibody, Dynabeads were first resuspended in the vial by vortexing for over 30 seconds. Appropriate numbers of the beads (165  $\mu\text{L}$  per  $10^9$  cells/mL) were transferred to a tube and placed on a magnet for one minute, after which the supernatant was discarded. Next, 1 mL of Buffer A (0.1 M Na-phosphate buffer, pH 7.4, made by dissolving 2.62 g  $\text{NaH}_2\text{PO}_4 \cdot \text{H}_2\text{O}$  and 14.42 g  $\text{Na}_2\text{HPO}_4 \cdot 2\text{H}_2\text{O}$  in distilled water to 1 L) was added to the beads, mixed, and separated on the magnet for another minute before discarding the supernatant. The tube was removed from the magnet, and the beads were resuspended in the same volume of Buffer A as the initial bead volume. After another magnetic separation for one minute and removal of the supernatant, 100  $\mu\text{g}$  of mouse anti-V5 tag antibody (Bio-Rad) was added, and Buffer A was added to reach a total volume of 150  $\mu\text{L}$ . The beads were mixed thoroughly either by vortexing or pipetting.

Afterward, 100  $\mu\text{L}$  of Buffer C (3 M ammonium sulfate dissolved in Buffer A, pH adjusted with NaOH or HCl to 100 mL) was added, and the beads were mixed again by vortexing or pipetting, followed by incubation on a roller at 37°C for 12–18 hours. Once the incubation was complete, the tube was placed on the magnet for 2 minutes, and the supernatant was removed. The beads

were washed with 1 mL of PBS (pH 7.4), with 0.05% Tween 20, mixed, and separated magnetically for 1 minute, and the supernatant was discarded. This wash step was repeated twice. The beads were then washed with 1 mL of PBS, followed by magnetic separation and discarding of the supernatant, repeating the washing step. Finally, the beads were resuspended in 240  $\mu$ L of 1X PBS to achieve a 20 mg/mL final bead concentration.

Cell lysis and protein capture were performed on tetracycline-induced (+Tet) and non-induced (-Tet, negative control) cells. A range of  $2 \times 10^6$  to  $1 \times 10^9$  cells was harvested by centrifugation at 1300 g for BF cells and 3000 g for PF cells, at 4°C for 10 minutes. The resulting pellet was resuspended in 10 mL of PBS containing protease inhibitors. Following a second centrifugation at 4°C for 8 minutes, the cell pellet was lysed in 1 mL of V5 IP buffer (20 mM Tris, pH 7.5, 150 mM KCl, 5 mM MgCl<sub>2</sub>, 0.05% IGEPAL, 0.5 mM DTT, and protease inhibitors). The cells were resuspended by pipetting and passed through a 21G  $\times$  1½ needle 20 times with a 1 mL syringe, followed by 20 passes through a 27G  $\times$  ¾ needle. The cell lysis was monitored under a light microscope for completeness. The sample was centrifuged at 10,000g for 15 minutes at 4°C, and the supernatant (lysate) was collected.

Since the proteins were attached to anti-V5 Dynabeads, the optimal method for native purification of RBP7910 and its protein partners was elution using V5 peptide competition. 50  $\mu$ L of V5 magnetic beads were washed with 1 mL of V5 IP Buffer, and the tube was placed on a magnet for 1 minute to discard the supernatant. The washing step was repeated twice. The cell lysate was then added to the beads and incubated at 4°C for 4 hours with rotation. After incubation, the tube was placed on a magnet for 1 minute to discard the unbound proteins. The

beads were washed twice with 1 mL of V5 IP Buffer. Finally, the beads were resuspended in 1 mL of PBS.

The supernatant was discarded for neutral elution of the target antigen after magnetic separation. 50 µL of 5 mg/mL V5 peptide (V7754-4MG (Sigma), prepared at 5mg/mL in PBS) was added to the beads, gently vortexed to mix, and incubated at 37°C on a rotator for 10 minutes. The beads were then separated on a magnet, and the supernatant containing the eluted antigen was collected. The elution step was repeated once for higher recovery. The three resulting eluates were then used for further analyses, such as WB and liquid chromatography mass spectrometry (LC-MS).

### ***8.9 Identification of RNA-dependent and -independent interacting protein partners of RBP7910-3V5***

LC-MS analysis was conducted to identify the RNA-dependent and -independent interacting partners of RBP7910-3V5 in BF and PF stages of *T. brucei*. This analysis was based on the three eluates obtained in the previous section under different conditions: -Tet (no induction), +Tet (induced), and +Tet+RNase (induced with RNase A treatment). The -Tet eluate was used as a negative control to exclude non-specific proteins that bound to the beads, while the +Tet eluate provided the complete set of proteins associated with RBP7910-3V5. The RNase A-treated eluate identified proteins that interact with RBP7910-3V5 through RNA.

To accurately identify the true protein interactions with RBP7910, the list of all identified proteins was processed through four distinct steps. First, the protein counts from both induced eluates were normalized relative to RBP7910. The identified proteins were annotated with their

corresponding gene IDs, names, and, where available, biological functions to enhance understanding of their roles. In the second step, proteins with fewer than two peptide counts were excluded. Next, protein counts in the non-induced eluate were subtracted to remove false positives from those in the induced samples. Additionally, proteins not localized in the mitochondrion—RBP7910's site of action—were removed using TritypDB (<https://tritypdb.org>) [77] as a reference.

The final step involved calculating the Normalized Spectral Abundance Factor (NSAF) for each identified protein. This calculation began by summing the spectral counts for each protein and dividing the total by the length of the protein to generate the Spectral Abundance Factor (SAF). The SAF values for each subunit in a multi-protein complex were then normalized by dividing each SAF by the total SAF values for all proteins within that sample, yielding the NSAF. The NSAF values represented the strength of interaction (edge length), while peptide counts reflected protein abundance. Protein abundance, derived from MS spectra counts, was normalized through the NSAF approach.

$$(\text{NSAF})_J = \frac{(\text{Sc}/L)_J}{\sum_{i=1}^N (\text{Sc}/L)_i}$$

Based on their NSAF values and relative abundance, proteins were categorized as either RNA-dependent or RNA-independent interactors. Protein-protein interaction networks were also generated using Cytoscape software, with the edges visually representing the relative abundance of the proteins.

## 8.10 Omics Data Collection and Analysis

Proteomic and transcriptomic data collection approaches were used to capture and quantify protein expression profiles across *T. brucei* life stages [71, 78]. This analysis aimed to identify mitochondrial RNA-processing genes exhibiting significant changes at the RNA or protein level during differentiation. Data preprocessing included normalization and statistical analysis to reduce noise and highlight proteins whose abundance varied distinctly between the SS, intermediate, and PF stages. Emphasis was placed on differentiating proteins involved in RNA-editing machinery and associated factors (e.g., gRNA-binding proteins), allowing a focused examination of stage-specific RNA processing.

### 8.10.1 Proteomic profiling of RNA editing machinery and the classification of RNA-processing complexes

Proteomic data generated by Dejung et al. (2016) at multiple time points during pleomorphic *T. brucei* BF-to-PF differentiation were reanalyzed to assess the abundance and variation of editosome proteins and related mitochondrial mRNA processing factors across key life stages. This analysis focused particularly on the transition from the short stumpy (SS) to the procyclic form (PF).

Mitochondrial RNA-processing proteins were categorized into four functional groups based on observed expression dynamics across life stages:

1. **Proteins upregulated during SS-to-intermediate stages:** Proteins like RBP7910, which are upregulated during SS-to-intermediate stages, indicate involvement in initial differentiation steps.

2. **Proteins upregulated throughout SS-to-PF stages:** Proteins upregulated throughout SS-to-PF stages may serve versatile roles in both differentiation and energy production.
3. **Proteins with peak abundance in the PF stage:** These proteins display peak abundance in the PF stage and are likely specialized for oxidative phosphorylation.
4. **Consistently downregulated proteins:** Proteins consistently downregulated, potentially acting to suppress early-stage differentiation signals.

To gain insight into the role of various editosome proteins in cell differentiation, we analyzed the potential functions of editosome proteins within each identified category, aiming to construct a hypothetical model of their sequential activity in mitochondrial RNA processing during *T. brucei* differentiation.

Our analysis reveals dynamic changes in protein abundance, while subsequent sections propose potential regulatory mechanisms that might control these changes during differentiation.

#### 8.10.2 Translational efficiency analysis in *T. brucei*

A key post-transcriptional regulatory mechanism, translational efficiency, significantly influences protein abundance across different life stages in *T. brucei*. Ribosome profiling was conducted in a study on BF and PF cells to assess translational efficiency across these stages [78]. We reanalyzed these available ribosome profiling data to investigate translational efficiency changes of editosome proteins during *T. brucei* differentiation. The dataset included ribosome-protected fragment sequencing (RPF-seq) and RNA-seq data from the BF and PF life stages, allowing for the assessment of translational efficiency specifically for proteins associated with

RNA editing complexes. Translational efficiency was the ratio of ribosome-protected fragment density to mRNA abundance for each gene, providing a measure of ribosome occupancy per transcript, while RNA stability had been also assessed in parallel using RNA-seq data from the same samples to determine the relationship between mRNA levels and translational efficiency.

### *8.10.3 RNAi Knockdown and Functional Analysis*

Available RNAi knockdown data [79] were analyzed to assess the functional roles of specific editosome components during differentiation. This included the silencing of selected editosome proteins, such as KREPA3 and KREP5, in both BF and PF *T. brucei*, to study their impact on cell viability, RNA editing activity, and protein complex stability.

### *8.10.4 Post-translational modifications and the role of RBPs*

Post-translational modifications (PTMs) also play a significant regulatory role in *T. brucei* protein expression. Among PTMs, protein phosphorylation can impact protein stability, subcellular localization, and enzymatic activity. A comprehensive MS-based phosphoproteomics study by Ferguson's group in 2013 revealed differential regulation of protein phosphorylation between the BF and PF stages of *T. brucei* [80]. We used existing phosphoproteomics data from BF and PF stages to elucidate PTM regulation in editosome proteins during differentiation. We also analyzed the regulatory roles of RBPs in RNA editing, examining their temporal expression patterns and interactions with editosome components.

### *8.10.5 Environmental stimulation for in vitro differentiation*

Simulating environmental cues such as cold shock, glucose deprivation, and kinase inhibitor treatments enabled *in vitro* examination of RNA-processing responses. By tracking mRNA

substrate editing levels under these conditions, it was possible to infer the influence of each environmental factor on RNA-editing enzyme activity. We assessed how these stimuli selectively modulate RNA-processing machinery by analyzing data on the editing levels of key mRNAs, such as COII and COIII across various environmental conditions [72], enhancing our understanding of environmental signal integration within *T. brucei*'s differentiation processes.

## 9. Results

**Objective 1. To analyze the role of RBP7910 in *T. brucei* differentiation from the BF to the PF cells at different time points by manipulating its expression.**

### *9.1 Optimization of direct BF to PF cell differentiation in monomorphic and pleomorphic *T. brucei**

In the initial phase of the project, direct BF to PF differentiation was optimized as a control to study the potential regulatory role of RBP7910 in cell differentiation. Both monomorphic SM427 and pleomorphic pHD1313 cells were extensively tested under varying conditions, including initial cell density (1 or 2 million cells/mL), timing of cold-shock induction (either at the start or 24 hours after induction), differentiation medium composition (using consistent SDM79, SDM80, and/or HMI-9 at different stages), and the addition of citrate and/or cis-aconitate at various concentrations (0 or 3 mM citrate, 3 or 6 mM cis-aconitate).

As shown in Table 3, all possible conditions were tested to identify the optimal combination, with Condition 14 being the most effective for BF to PF differentiation. For optimal results, an initial density of approximately 1 million cells/mL should be incubated in HMI-9 medium, supplemented with 3 mM citrate and 6 mM cis-aconitate at 37°C for 24 hours. Following this, the medium should be replaced with SDM79 and incubated at 27°C for at least 48 hours to allow for the morphological changes associated with PF cells to emerge (see Fig. 7). EP procyclin expression, a specific marker for PF cells, can be detected after 48 hours (Fig. 8).

**Table 3. Results of optimization for the direct BF to PF differentiation in monomorphic and pleomorphic *T. brucei***

Condition no.	Initial cell density (M cells/ml)		Differentiation medium*			Growth medium**			Cis-aconitate Conc. (μM)		Citrate Conc. (μM)		Time of medium exchange (h)		Results***
	1	2	HMI-9	SDM-79	SDM-80	HMI-9	SDM-79	SDM-80	3	6	0	3	0	24	
1		■		■			■			■	■		■		XX
2	■			■			■			■	■		■		X
3	■				■			■		■	■		■		XXX
4	■			■				■		■	■		■		XXX
5	■				■			■		■	■		■		XXX
6	■		■					■		■	■		■		✓
7	■		■					■		■	■		■		✓✓
8		■	■					■		■	■		■		✓
9	■		■					■		■	■		■		X
10	■			■				■		■	■		■		XX
11	■			■				■		■	■		■		XXX
12	■				■			■		■	■		■		XXX
13	■				■			■		■	■		■		XXX
14	■		■					■		■	■		■		✓✓✓
15	■		■					■		■	■		■		✓✓
16		■	■					■		■	■		■		✓✓

\* Initial medium for differentiation induction (0-hour): Specifies the medium used to initiate differentiation, including HMI-9, SDM-79, or SDM-80.

\*\* Medium for culturing induced cells (24-hour): Indicates the medium used for the continued growth of cells after 24 hours, including HMI-9, SDM-79, or SDM-80.

\*\*\* Differentiation and Viability Results: Outcomes of differentiation induction are represented as follows:

XXX Very low viability, not differentiated

XX Low viability, not differentiated

X Not differentiated

✓ Differentiated, poor viability

✓✓ Differentiated, good viability

✓✓✓ Highly differentiated, good viability

The black colour indicates the selected factor for each specific variable.

Abbreviations: M: million cells, Conc: concentration; h: hour

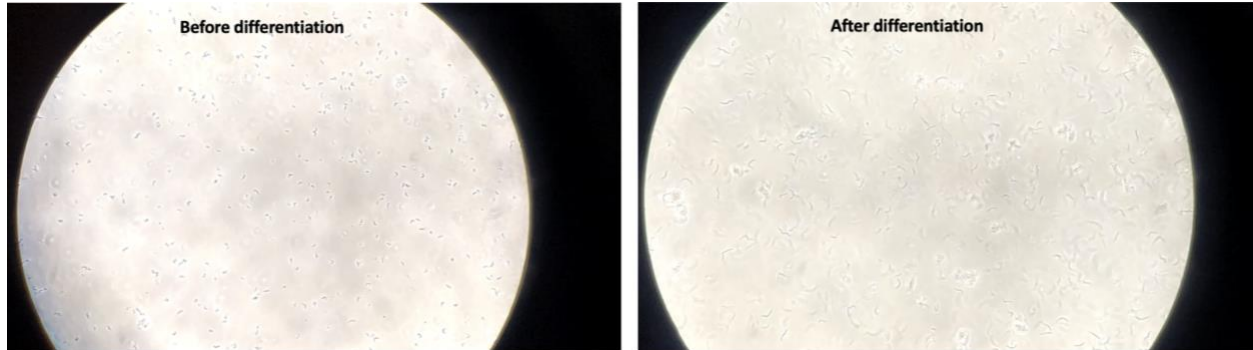


**Fig. 7 Morphological changes during direct BF to PF cell differentiation in monomorphic and pleomorphic *T. brucei*.** Cells were imaged at various stages of the differentiation protocol, highlighting the transition from BF to PF stage after treatment with cis-aconitate and cold shock. PF cells (right) display characteristic elongated morphology with a long, slender body and an extended flagellum, as shown in the optimized differentiation condition.

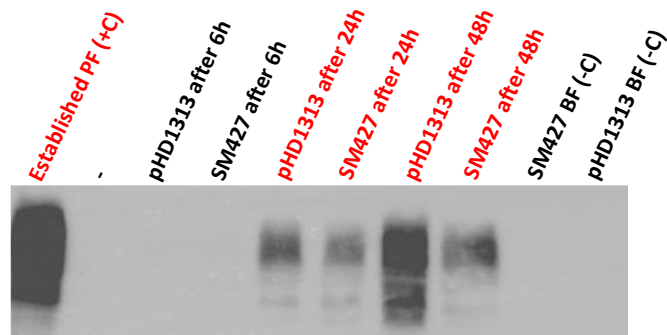


**Fig. 8 Expression of EP procyclin as a marker of PF differentiation by induced monomorphic and pleomorphic *T. brucei*.** Western blot analysis demonstrates the presence of EP procyclin starting at 24 hours post-induction by the cells subjected to the optimized BF to PF differentiation protocol, confirming the successful transition to the PF stage.

*Abbreviations:* +C: positive control; -C: negative control; h: hours

### **9.2 Indirect BF to PF cell differentiation in pleomorphic *T. brucei***

The successful indirect induction of BF pleomorphic *T. brucei* (pHD1313 cells, a gift from C. Clayton, Heidelberg University) into PF through the SS form, the specialized transmission stage,

was achieved. Cells were first cultured in 1.1% methylcellulose-containing complete HMI-9 medium at 37°C with 5% CO<sub>2</sub> for 48 hours to promote SS formation. This allowed for more synchronized responsiveness to the CCA signals for the next PF differentiation step, which is provided via specific expression of PAD1 by SS cells. PAD1 is a protein from the carboxylate surface transporter family (PAD proteins), predominantly expressed at significant levels during the SS stage. Therefore, the transition from LS to SS was confirmed by studying the expression of PAD1 by the induced cells after 48 hours (Fig. 9).

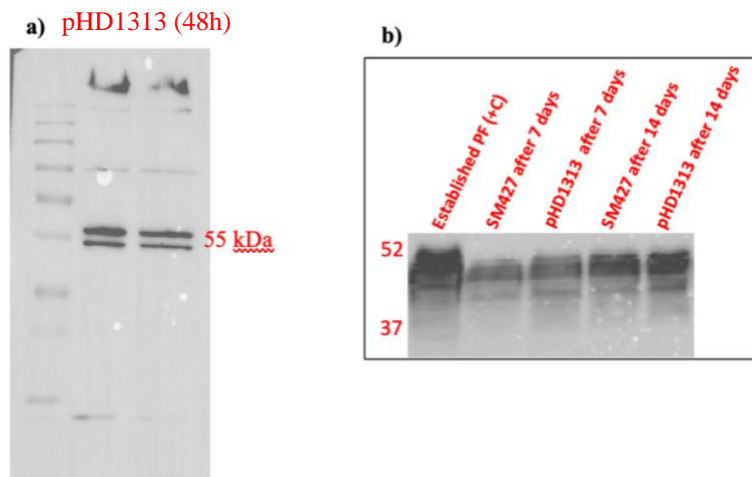


**Fig. 9 Induction of indirect BF to PF cell differentiation in pleomorphic *T. brucei* cell line.** PAD1 expression, a marker of BF stumpy cells, indicates successful induction into the transmission stage, enabling responsiveness to CCA signals for subsequent PF differentiation (a). Confirmation of BF to PF differentiation in pleomorphic *T. brucei* through the SS stage. Western blot analysis shows the expression of EP procyclin, in induced cells through the SS stage following incubation with CCA and cold shock. Expression of EP procyclin was stable up to two weeks post-induction, confirming successful differentiation (b).

Following SS formation, cells were induced to differentiate into PF by incubation in HMI-9 medium with CCA at 37°C for 24 hours, followed by incubation in SDM79 medium at 27°C for an additional 48 hours, leading to morphological changes characteristic of PF cells. Figure 9b presents the WB results, confirming the successful BF to PF differentiation through the SS stage,

with stable cell growth and sustained expression of EP procyclin observed two weeks post-induction.

### 9.3 Transfected monomorphic BF SM427 cells expressed V5-tagged RBP7910

To study the effect of RBP7910 on cell cycle progression, BF *T. brucei* SM427 cells were transfected with an RBP7910 gene tagged with V5 using the pLew100 plasmid [76]. RBP7910 was overexpressed in cells that may also express the endogenous form. Cells not treated with tetracycline served as a negative control, with no ectopic RBP7910-3V5 expression while increasing tetracycline levels led to robust protein expression in the induced cells (Fig. 10)

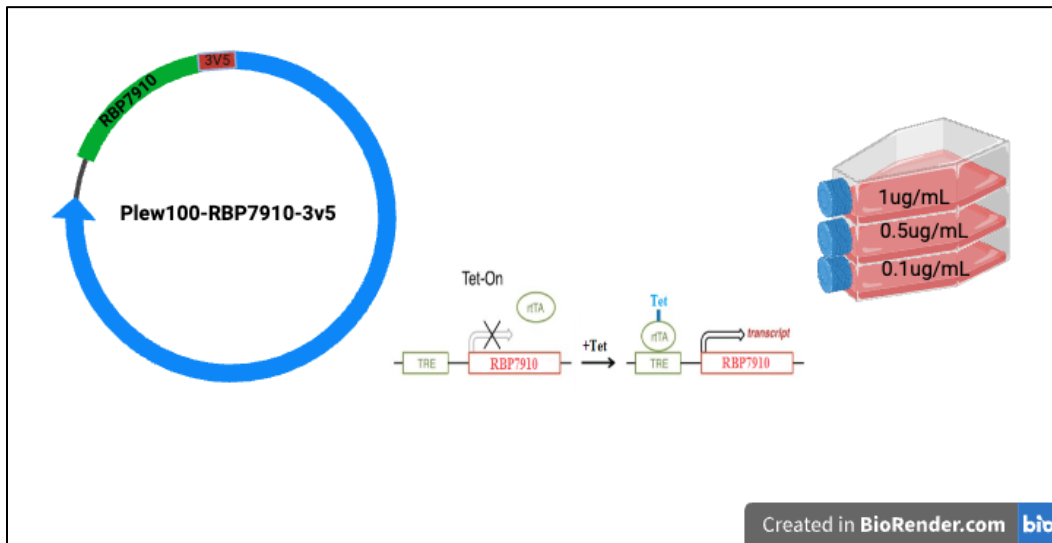


**Fig. 10 Schematic view of RBP7910 overexpression in SM427-plew100-RBP7910-3V5 cell line.** Various concentrations of tetracycline including 0.1, 0.5, and 1 µg/mL were performed to induce RBP7910 overexpression in the cells.

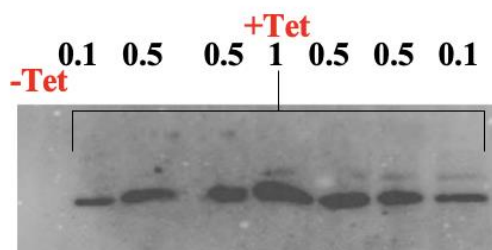


**Fig.11 Tetracycline-induced expression of V5-tagged RBP7910 in monomorphic BF *T. brucei* SM427 cells.** Western blot analysis shows robust expression of RBP7910-3V5 in tetracycline-treated cells (+Tet), while untreated cells (-Tet; negative control) show no ectopic expression.

#### ***9.4 Overexpression of RBP7910 in monomorphic BF *T. brucei* induces changes resembling PF differentiation***

Significant cellular and molecular changes were observed following RBP7910 OE in monomorphic BF *T. brucei*, resembling the differentiation towards the PF stage. These changes are similar to those induced by CCA treatment and cold shock. First, fluorescence microscopy revealed that mitochondria were significantly larger in several cells within the induced culture (+tet) than in uninduced cells (-tet) (Fig. 12) [76]. In these induced cells, mitochondrial structures appeared more developed than PF cells. Uninduced control cells, which were not treated with tetracycline, exhibited no overexpression of RBP7910, while the induced cells displayed enlarged mitochondria with enhanced cristae formation. This suggests that RBP7910 overexpression may influence RNA editing and promote the expression of specific electron transport chain proteins typically produced only in PF cells. Consequently, RBP7910 OE may impact mitochondrial RNA processing and support the expression of components required for mitochondrial respiration, similar to what occurs in PF cells.

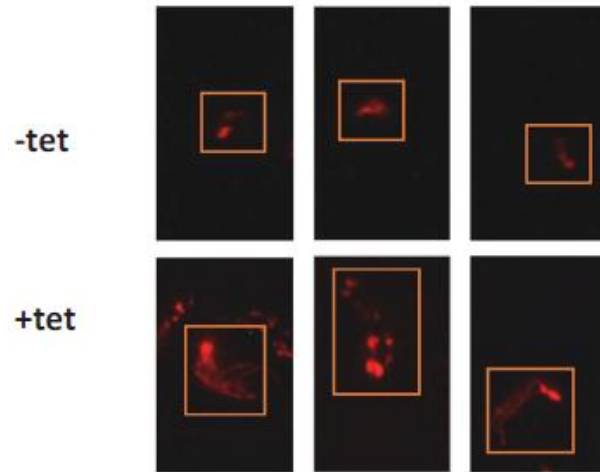


**Fig. 12 Overexpression of RBP7910 in BF cells results in more developed and enlarged mitochondria [76]. <https://escholarship.mcgill.ca/concern/theses/cv43p283j>**

A comprehensive analysis was conducted to assess RBP7910's potential regulatory effects on the cell cycle progression of monomorphic BF *T. brucei* (Fig. 13). Figure 13 presents eight distinct experimental conditions used to assess the impact of RBP7910 overexpression on the differentiation of BF parasites, alongside known inducers like CCA treatment and cold shock, both established triggers for BF-to-PF differentiation *in vitro*. This study further investigates possible synergistic or inhibitory interactions between RBP7910 and these differentiation inducers.

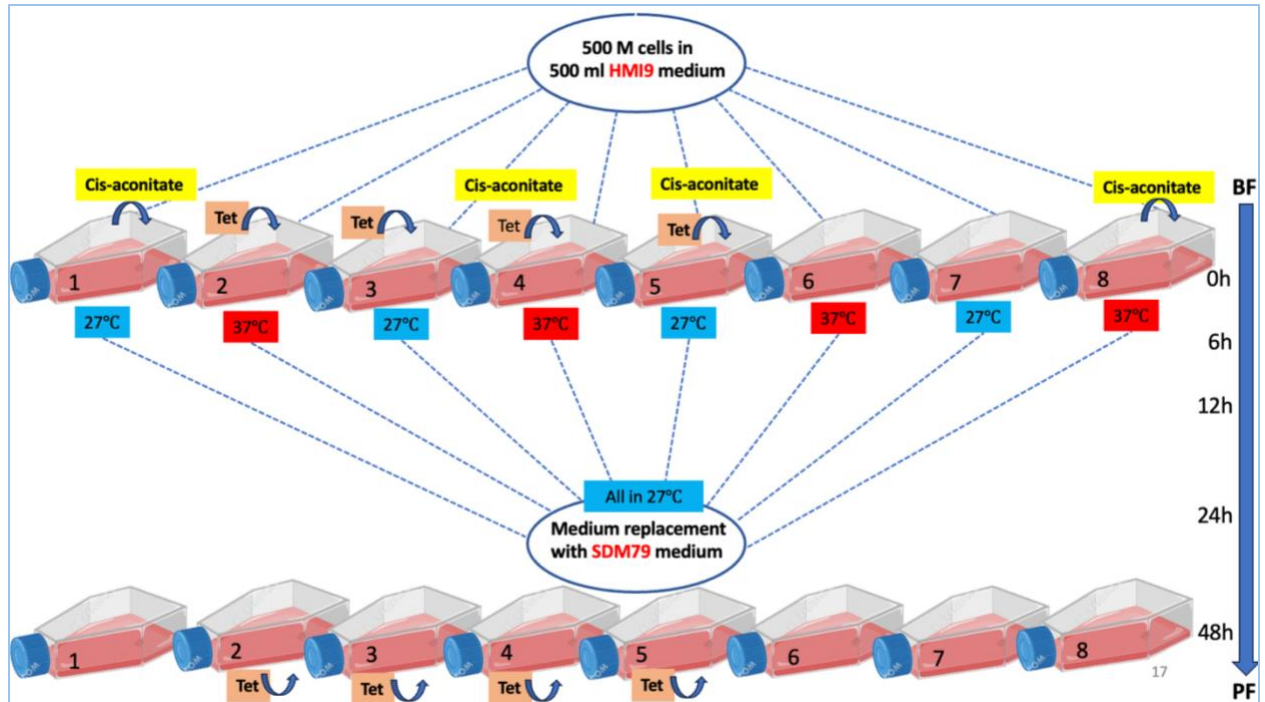


**Fig.13 Experimental setup to assess the impact of RBP7910 overexpression on cell cycle progression in monomorphic BF *T. brucei*.** Eight distinct conditions were designed, combining RBP7910 overexpression, CCA treatment, and cold shock, to evaluate their individual and combined effects on differentiation and EP procyclin expression.

*Abbreviation:* Tet: tetracycline; h: hours

WB analysis of EP procyclin, a protein marker for PF *T. brucei*, showed that cells overexpressing RBP7910 began expressing EP after 48 hours of induction (Fig. 14a; C2-48h), whereas uninduced cells did not express EP at any time point (Fig. 14c; C6-0-48h). As illustrated in Figure 14a, RBP7910 overexpression alone compensates for the absence of CCA treatment or cold shock, effectively inducing EP procyclin expression. Results also indicated that while CCA treatment alone can induce EP procyclin expression within 24 hours, cold shock alone cannot achieve this (Fig. 14d; C7 and C8, respectively). Thus, although a 10°C cold shock supports

differentiation in cells overexpressing RBP7910, it is not the primary driver of BF-to-PF differentiation.

WB analysis for conditions 4 and 8 (Fig. 14b and 14d) revealed that treated cells began expressing EP protein 24 hours before being exposed to cold shock, suggesting that RBP7910 initiates EP procyclin expression and differentiation through a mechanism similar to CCA. Moreover, while cold shock alone does not result in EP expression (Fig. 14d; lanes 6, 7, 8, and 9), it does enhance EP induction in RBP7910-overexpressing cells, with expression observed only after 48 hours when cold shock is applied (see 24- and 48-hour time points in Fig. 14a, 14b, and 14d). Interestingly, EP is not expressed at any time (12–48 hours) when cold shock is applied concurrently with RBP7910 overexpression from the start (Fig. 14b; C3). This finding suggests that, while cold shock aids RBP7910-mediated differentiation, an unknown inhibitory effect may prevent EP expression when both RBP7910 overexpression and cold shock are initiated simultaneously (Fig. 14a and b; conditions 2 and 3).

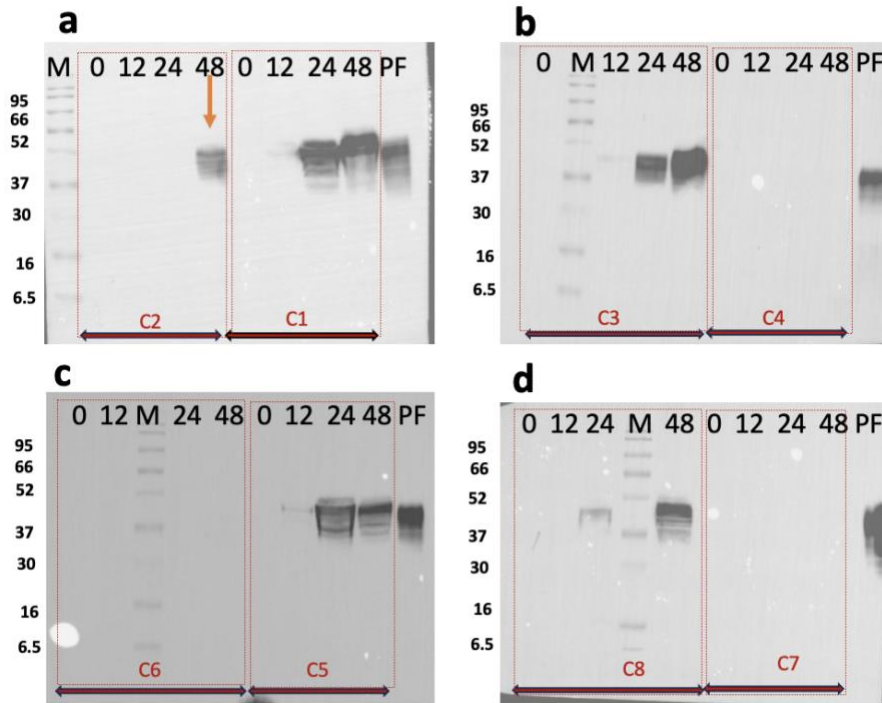


**Fig. 14 Western blot analysis showing EP procyclin expression in response to RBP7910**

**overexpression, CCA treatment, and cold shock in BF *T. brucei*.** RBP7910 overexpression alone induces EP expression within 48 hours, compensating for the absence of CCA or cold shock. CCA alone induces EP expression within 24 hours, while cold shock enhances EP induction but does not independently trigger it. Control cells without RBP7910 overexpression or treatment do not express EP at any time point.

*Abbreviations:* C: condition, M: marker; 0,12,24,48: time-points per hour; CA: cis-aconitate; Procyclic form (PF): Established PF cells expressing EP procyclin, serving as a positive control for differentiation and EP expression.

Finally, our results show that RBP7910 overexpression enhances CCA-induced EP expression, as a stronger signal was observed at 48 hours in conditions 4 and 5 compared to conditions 8 and 1 (without RBP7910 overexpression).

Figure 15 further confirmed that EP expression in condition 2 results from RBP7910 overexpression, as tagged RBP7910 expression was detected only in tetracycline-induced cells (Fig. 15; C2-5).

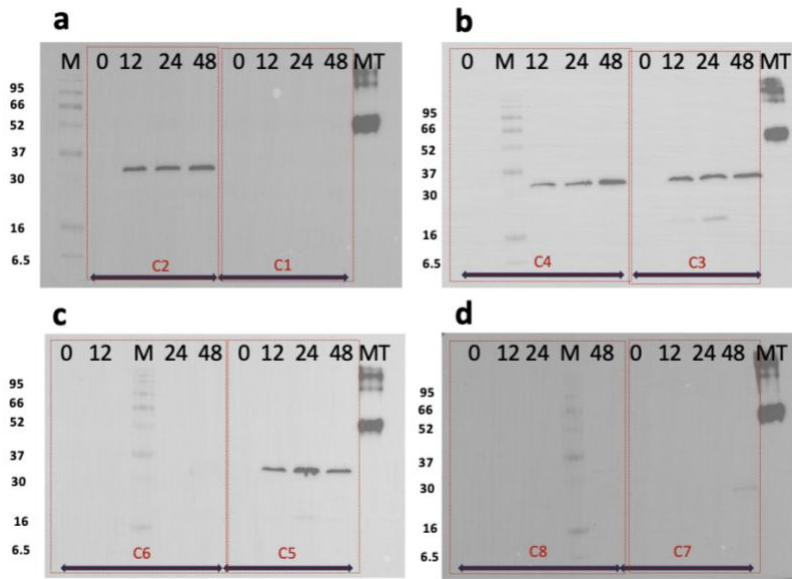


**Fig. 15 Confirmation of RBP7910 overexpression in the tetracycline-induced cells.** V5-tagged RBP7910 expression was detected only in tetracycline-induced cells (C2-5), correlating with the observed EP procyclin expression in BF *T. brucei*. This demonstrates the direct role of RBP7910 in enhancing CCA-induced differentiation.

*Abbreviations:* C: condition; M: marker; 0,12,24,48: time-points per hour; CA: cis-aconitate; MT: multi-tag protein serving as positive control for V5 tag expression

**Objective 2. To distinguish between RNA-dependent/independent protein-protein interactions of RBP7910 during the differentiation of *T. brucei* from BF to PF**

***9.5 Immunoprecipitation of V5-tagged RBP7910***

In a previous study conducted by our lab, both RNA-dependent and RNA-independent protein partners interacting with RBP7910 in the PF stage of *T. brucei* had been examined (Fig. 16) [76]. Figure 14 illustrates the WB results from the IP experiments, with three panels representing different conditions: the first panel (negative control) shows no protein detection without tetracycline induction; the second panel shows results with tetracycline-induced RBP7910-3V5 expression; and the third includes an RNase A treatment, which removes proteins bound indirectly to RBP7910-3V5 via RNA, leaving only direct protein interactions.

To further characterize these interactions across life stage transitions, this study investigates RBP7910 protein partners in the BF stage of *T. brucei*, with and without RNase treatment. Native RBP7910 and its partners were isolated from BF *T. brucei* cell lines expressing RBP7910-3V5, induced with 0.5 µg/mL tetracycline for 24 hours. IP experiments used anti-V5 magnetic beads, and V5 peptide competition was chosen as the elution method to preserve native protein interactions.

Three experimental conditions were tested: (1) without tetracycline induction (-Tet; no RBP7910-3V5 expression), (2) with tetracycline induction but without RNase treatment (+Tet/-RNase; induced expression of RBP7910-3V5), and (3) with both tetracycline induction and

RNase A treatment (+Tet/+RNase A; induced expression with RNA-independent interactions preserved). WB results for these IP experiments performed in BF cells are shown in Figure 15. Eluates from these three conditions were further analyzed by mass spectrometry (MS) to identify and characterize RBP7910 protein partners in the BF stage, providing a comparison to the previously analyzed PF cell interactions.

a)

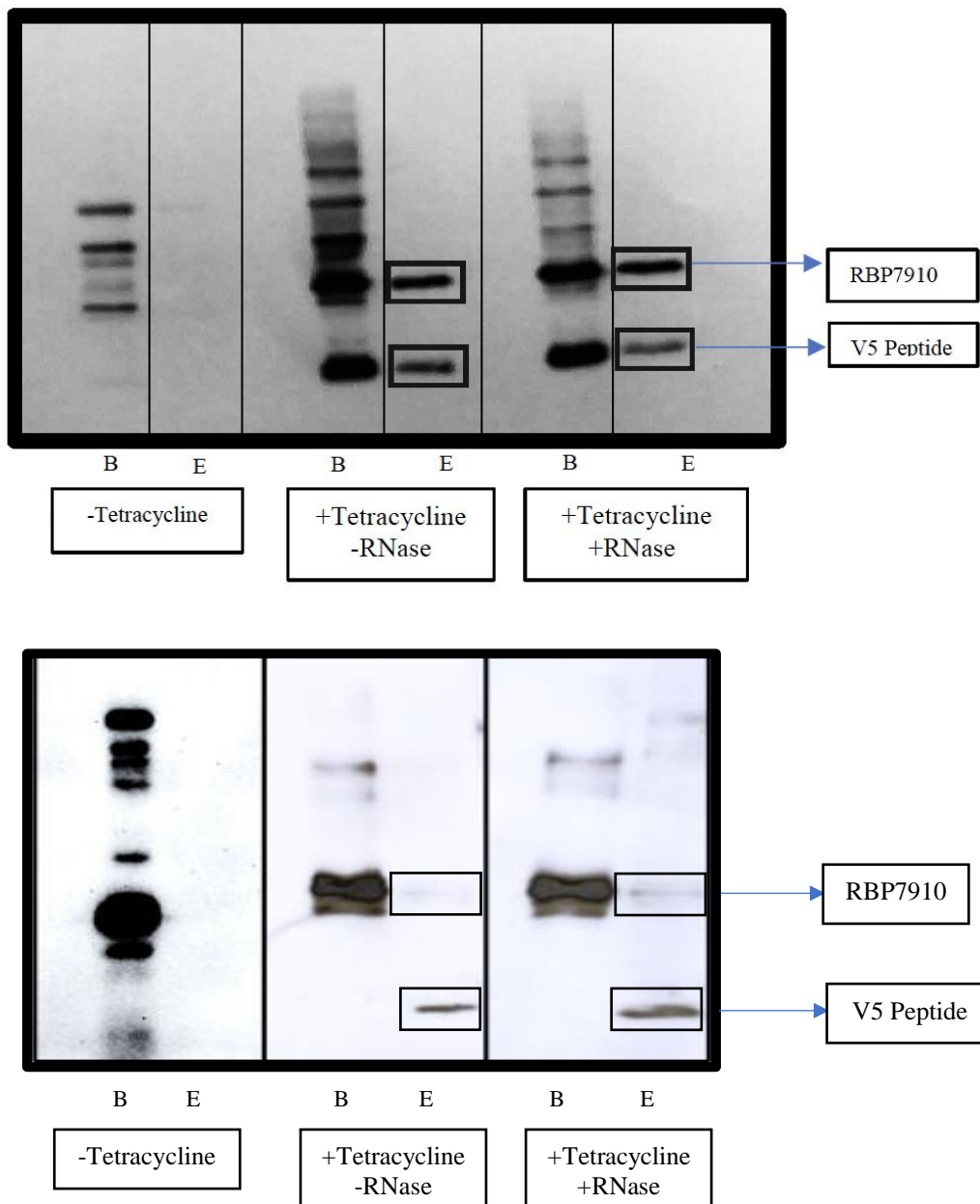


**Fig.16 Purification and analysis of V5-tagged RBP7910 interacting partners in the PF (top) and the BF (bottom) *T. brucei*, with and without RNase treatment.** IP was performed using anti-V5 agarose and anti-V5 magnetic beads for the PF (top) [76] and BF (bottom) cells, respectively, with elution achieved through V5 peptide competition. WB analysis displays three conditions for both BF and PF parasites: (a) - Tet, no tetracycline induction (no RBP7910-3V5 expression); (b) +Tet/-RNase, with tetracycline induction (RBP7910-3V5 expressed, no RNase treatment); and (c) +Tet/+RNase A, with tetracycline induction and RNase A treatment (RBP7910-3V5 expressed, preserving RNA-independent interactions). Blue arrows indicate the positions of the RBP7910-3V5 protein and V5 peptide.

*Abbreviations:* B: proteins bound to the beads; E: final eluted fractions.

### ***9.6 Mass spectrometry profiling of RBP7910-3V5: Characterization of RNA-mediated and direct protein interactions***

The three eluates prepared from BF in the previous step were analyzed using Liquid Chromatography-Mass Spectrometry (LC-MS). The eluate without tetracycline induction acted as a control to filter out nonspecific binders, while the second eluate (tetracycline-induced) provided a complete list of proteins interacting with RBP7910-3V5. The third eluate, treated with RNase A, identified proteins bound to RBP7910-3V5 via RNA.

Approximately 100 proteins were analyzed through a multi-step process explained in the method section to accurately identify RBP7910's true interactors. Protein counts in both induced eluates were normalized to RBP7910 count and annotated with gene IDs, names, and functions. Proteins with fewer than two peptide counts were excluded, and false positives were filtered out using the control eluate and mitochondrial localization data from TriTrypDB [77]. Finally, Normalized Spectral Abundance Factor (NSAF) values were calculated to classify interactors as RNA-dependent or RNA-independent. The final list of rigorously verified protein interactors is presented in Table 2, with the complete list from this IP experiment available in Appendix 1.

**Table. 4 Classification of RBP7910 interacting proteins in *T. brucei* BF identified by LC-MS analysis**

Identified Proteins	Accession Number	Normalized RNase+	Normalized RNase-	Length	SAF RNase+	SAF RNase -	NSAF RNase +	NSAF RNase -
Ribosomal protein L3, mitochondrial, putative	Q581Q1	46.5	6	429	0.108391608	0.013986014	0.01808595	0.009464228
Intraflagellar transport protein-like protein	Q57WF2	24	13	596	0.040268456	0.021812081	0.006719093	0.014760068
glycerol kinase	Q38DE9	2	2	512	0.00390625	0.00390625	0.000651787	0.002643329
Uncharacterized protein	Q38AH3	3	3	189	0.015873016	0.015873016	0.002648531	0.010741148
Mitochondrial RNA binding protein	Q57Y20	1.5	4	915	0.001639344	0.004371585	0.000273537	0.002958218
Ubiquitin-activating enzyme E1, putative	Q38DE8	0	8	1214	0	0.006589786	0	0.004459258
Guide RNA associated protein, GAP2	Q57XL7	0	4	473	0	0.00845666	0	0.005722557
RNA-binding protein, putative	Q389P7	0	1	320	0	0.003125	0	0.002114664
Guide RNA associated protein, GAP1	Q586X1	0	3	492	0	0.006097561	0	0.004126173
Mitochondrial RNA binding complex 1 subunit	Q57WL2	0	3	934	0	0.003211991	0	0.00217353

Cytoscape software was utilized to construct a protein-protein interaction (PPI) network, with edge thickness visually representing protein abundance. Interacting partners were categorized as RNA-dependent and RNA-independent proteins (Fig. 17), enabling a clear visualization of RBP7910's interaction landscape. This categorization facilitated further insights into RBP7910's role in RNA processing and mitochondrial function in *T. brucei*.

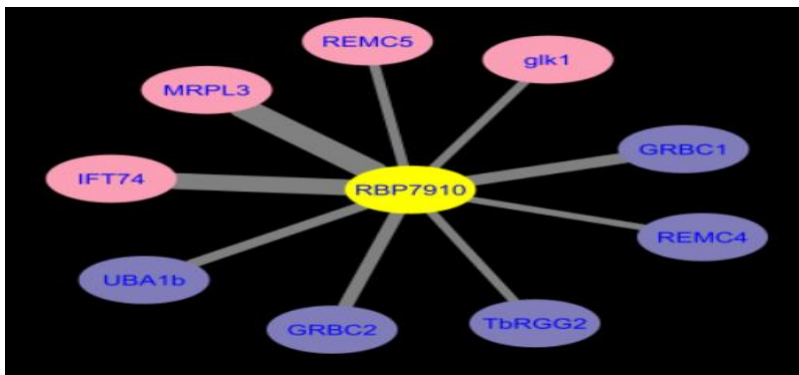
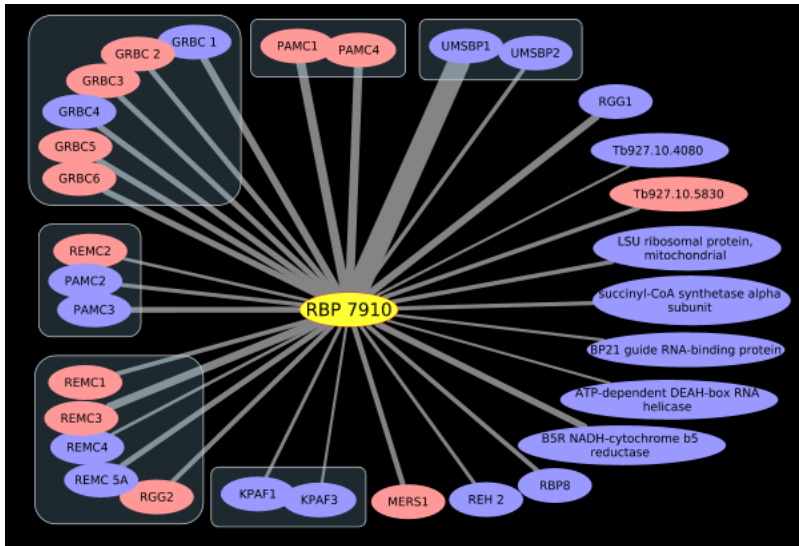


**Fig. 17 Cytoscape PPI network analysis of RBP7910 interacting partners in the PF (top) and the BF (bottom) *T. brucei*, based on LC-MS analysis of three eluates.** Interacting partners of RBP7910 were identified in the PF [76] and BF parasites. The eluate without tetracycline induction served as a control to filter out nonspecific binders. The tetracycline-induced eluate identified the complete set of RBP7910-3V5 interactors, while the RNase A-treated eluate distinguished RNA-independent (pink nodes) and RNA-dependent interactions (violet nodes, absent after RNase treatment). Edge thickness also represents relative protein abundance.

### **Objective 3. To investigate the adaptive mechanisms governing mitochondrial RNA processing across *T. brucei* life stages**

This part of study synthesizes available omics data to examine how environmental cues and protein complexes coordinate stage-specific RNA-editing and processing adaptations. Focusing on regulatory changes during the SS-to-PF transition, we aim to identify key RNA-processing proteins that enable *T. brucei* to differentiate and adapt for survival in both mammalian and insect environments.

#### ***9.7 Editosome protein Abundance profile During SS-to-PF Differentiation***

An analysis of available proteomics data from *T. brucei* during BF-to-PF differentiation identified four main groups of RNA-processing proteins with distinct expression patterns [71], as summarized in Table 5:

1. **Upregulated during SS-to-PF differentiation:** Includes RBP7910 (from the RESC family), KRBP16 (RBP16) from auxiliary factors, and some other associated members of editing holoenzymes.
2. **Upregulated both during SS-to-PF differentiation and in the PF stage:** Includes proteins such as KREPA3 (from the RECC family) and RESC13 (TbRGG2), showing SS and PF stages.
3. **Specifically upregulated in the PF stage:** Includes KRET2 (RET2) and MEAT1 among the RECC and auxiliary factors, respectively, with expression solely elevated in the PF stage.
4. **Downregulated Proteins:** Includes proteins like KREPB4 (RECC family of proteins) that exhibited reduced abundance during BF-to-PF differentiation.

Our findings demonstrate significant distinct profiles in editosome protein abundance and functionality between the BF and PF life stages.

**Table. 5 Expression patterns of mitochondrial RNA-processing proteins during SS to PF differentiation in *T. brucei***

TriTryp ID	Legacy		Assigned	Complex name	Time points of differentiation from Bf to PF									
					LS	SS	2h	4h	6h	12h	24h	48h	PF	
Tb927.11.2990	MP46	KREPB4	KREPB4	RECC										
Tb927.4.4160	REMC5	MRB4160	RESC12	RESC										
Tb927.8.620	MP42	KREPA3	KREPA3	RECC										
Tb927.10.7910	MERS3	RBP7910	RESC19	RESC										
Tb927.7.3950	RET1	KRET1	KRET1	MPsome										
Tb927.11.9150	MPSS1		MPSS1	MPsome										
Tb927.10.9000	MPSS2		MPSS2	MPsome										
Tb927.6.1680	H2F1	MRB1680	KH2F1	REH2C										
Tb927.2.1860	REMC2	MRB1860	RESC9	RESC										
Tb927.11.8870	REH1	mHEL61	KREH1	Auxiliary										
Tb927.11.7900	RBP16		KRBP16	Auxiliary										
Tb927.4.1500	REH2		KREH2	REH2C										
Tb927.9.12770	KPAF3		KPAF3	KPAC										
Tb927.10.10830	TbRGG2	TbRGG2	RESC13	RESC										
Tb927.8.8180	REMC4	MRB8180	RESC11A	RESC										
Tb927.2.2470	MPS1	KREPA1	KREPA1	RECC										
Tb927.10.1730	PAMC3		RESC17	RESC										
Tb927.10.9720	REAP-1		KREAP1	Auxiliary										
Tb927.1.1330	MEAT1		MEAT1	Auxiliary										
Tb927.11.14380	KPAF2		KPAF2	KPAC										
Tb927.6.2140	H2F2		KH2F2	REH2C										
Tb927.7.1550	RET2	KRET2	KRET2	RECC										
Tb927.7.800	REMC3	MRB800	RESC10	RESC										
Tb927.9.4360	REL1	KREL1	KREL1	RECC										
Tb927.6.1200	PAMC2		RESC16	RESC										
Tb1.02.5390	GRBC4	MRB5390	RESC4	RESC										
Tb927.1.3010	PAMC4		RESC18	RESC										
Tb927.9.7260		MRB7260	RESC14	RESC										

Black: Significantly upregulated

White: Significantly downregulated

Gray: Not regulated

Proteins were regulated if their fold change was greater than 2 and their P value was less than 0.05.

Adopted from [71].

Abbreviations: BF: Blood form, PF: Procycliv form, LS: Long slender, SS: Short stumpy, h: hour.

Kinases like CK2A2 and NEK12.2 also display stage-specific regulation that may influence differentiation through metabolic signalling [70]. Their expression patterns correlate with responses to cold shock and glucose variation, with the cold-shock-induced editing of COII and COIII further emphasizing their regulatory role in BF-to-PF differentiation [72].

Figure 18 presents a comparative expression profile of the mitochondrial RNA-processing and kinase activity proteins [70]. Box plots illustrate the expression patterns for non-editing RNA-processing proteins (Figure 18a), while Figure 18b highlights kinase activity profiles over time, offering a clear view of the shifts in protein abundance across differentiation stages. The distribution of log<sub>2</sub> abundances within each boxplot clarifies protein regulatory dynamics at various time points, reinforcing the observed trends in protein abundance for specific protein groups.

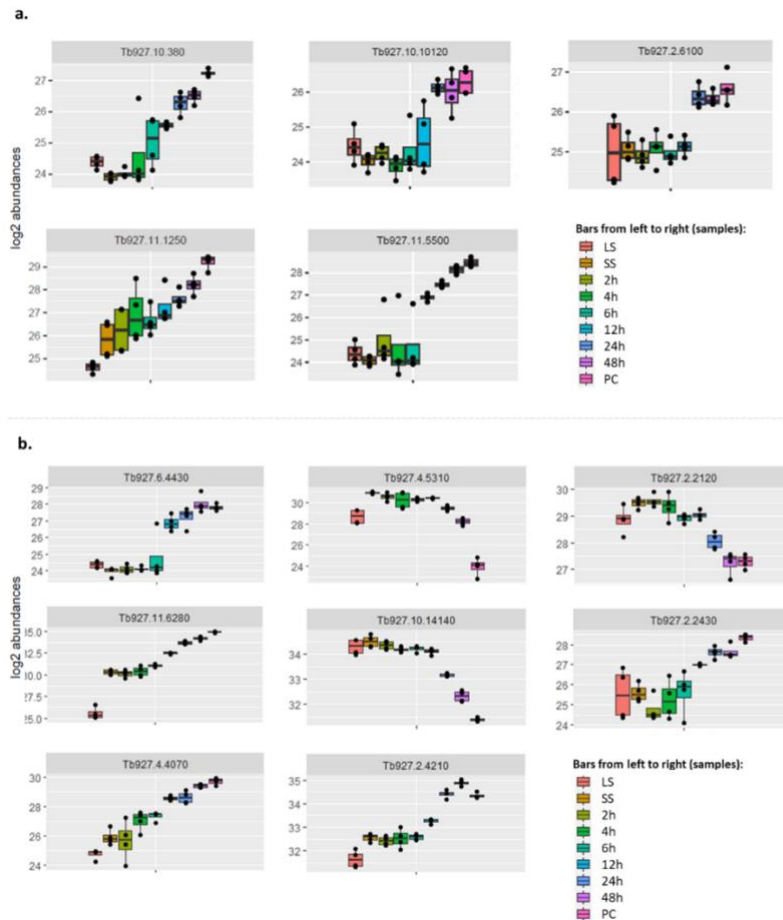


**Fig. 18 Comparative expression profiles of mitochondrial mRNA processing and kinase activity proteins during BF to PF differentiation in *T. brucei*.** Box plots illustrate the expression profiles of proteins in (a) mitochondrial mRNA processing (excluding editing proteins) and (b) kinase activity Gene Ontology (GO) groups. Each boxplot represents protein abundance across different time points with four replicates per time point. The height of each box indicates the distribution of log<sub>2</sub> abundances, with the line inside denoting the median value. Kinases such as CK2A2 and NEK12.2 exhibit stage-specific regulation, aligning with cold shock and glucose variation responses, highlighting their potential regulatory role in BF-to-PF differentiation.

### **9.8 Translational Efficiency in *T. brucei***

Translational efficiency, a key post-transcriptional regulatory mechanism, significantly influences protein abundance across *T. brucei* life stages [78]. Our ribosome profiling analyses of the available data [78] revealed life-stage-specific regulation, where translational efficiency often operates independently of RNA stability, underscoring distinct control mechanisms at the translational level. In the PF stage, RESC complex members, such as RESC16 (PAMC2), TBRGG2, and RESC14 (MRB7260), rank in the top 5% of genes with increased translational efficiency compared to the BF stage. This increase likely supports the enhanced mitochondrial RNA editing needs in PF by facilitating gRNA-mRNA interaction through RESC proteins.

Additional components, including RESC4 (GRBC4), KREH2 (from the REH2C complex), KPAF1 (from the KPAC complex), and MEAT1 (Auxiliary factors), also exhibited high translational efficiency, positioning them within the top 10% of upregulated genes. In contrast, selected RECC complex members, specifically KREPB9 and KREPB5, along with the auxiliary factor KREAP1, displayed reduced translational efficiency in PF, indicating decreased functionality or regulation of these proteins in the PF stage.

### **9.9 Role of RNA Binding Proteins**

To explore additional regulatory mechanisms of editosome proteins during *T. brucei* differentiation, we retrieved a list of RBPs in *T. brucei brucei* from TriTrypDB [77] using the Gene Ontology (GO) term “RBP.” Expression profiles for these RBPs were then obtained from Janzen’s study [71] to identify proteins with regulatory patterns during differentiation (see Appendix 2 for the full list of RBPs alongside their expression profile during BF-to-PF differentiation).

To identify potential RNA targets of these RBPs, we searched the CISBP-RNA database (catalogue of inferred sequence binding preferences for RNA) (<http://cisbp-rna.cabr.utoronto.ca/>). for RBPs with known binding sequences. As no *T. brucei brucei* data was available, we identified the orthologs of these RBPs in *T. brucei gambiense* and cross-referenced them with the *T. brucei gambiense* RBP list in CISBP-RNA. Of the thirteen RBPs in this database with inferred sequence binding preferences, only one —Tb927.3.3960 (DRBD6A, or double RNA binding domain protein 6A) —was found to have an inferred binding motif (CAUa/uGU) and showed significant regulation during differentiation, starting at the 12-hour time-point and continuing into the PF stage.

A motif search identified similar sequences in the 3' or 5' UTRs of all editosome proteins as potential targets of this DRBD6A during differentiation. This search identified twelve proteins, containing the motif (CAUa/uGU): **KRET2**, **RESC17**, RESC2, KREN1, KREPA5, KREPB7, **KRBP16**, **RESC11**, MPSS3, MPSS4, **KREPA3**, and **RESC10**. Among these, KREN1, KREPA5, KREPB7, and MPSS3 were not detected in Janzen's study and RESC2 and MPSS4 showed no significant change during SS-to-PF transition, indicating a lack of regulation during differentiation. The remaining proteins (in bold) demonstrated differential regulation at various time points or in the PF stage, suggesting they may be targeted by DRBD6A through their 3' or 5' UTRs.

### **9.10 *Post-translational modifications in Gene Expression Regulation***

Protein phosphorylation emerged as a significant PTM affecting gene expression in *T. brucei*, influencing factors such as stability, subcellular localization, and enzymatic activity. A SILAC-based phosphoproteomic study [81] showed differential regulation of phosphorylation between BF and PF stages, with the majority being phosphoserine (80%), followed by phosphothreonine (17%) and phosphotyrosine (3%). This phosphorylation pattern aligns with functions tied to motility, protein kinase activity, and gene expression regulation.

Notably, none of the identified phosphorylation sites in editosome proteins were specific to either BF or PF stages, indicating a stable phosphorylation profile across life stages. An exception was KMRP1, a gRNA-binding protein, which showed over tenfold upregulation of phosphorylation in PF. While KMRP1's regulation did not significantly impact differentiation directly, it suggests a potential role for phosphorylation in fine-tuning of RNA-protein interactions during this transition. The lack of significant phosphorylation variation in editosome proteins highlights the need for further exploration of other PTMs that may interact with RBPs, potentially modulating editosome function in response to life-stage-specific cues.

### **9.11 *The role of RNA Editing and Environmental Cues in Mitochondrial RNA Processing***

Transcriptomic studies also showed that edited transcript levels of key cytochrome mRNAs, such as COII and Cyb, increased significantly during differentiation [72]. This increase aligns with protein abundance profiles, suggesting stage-specific regulatory mechanisms. The selective response to environmental stimuli underscores an intricate network adapting mitochondrial function to host-vector transitions.

Cold shock and glucose restriction were found to influence the expression of mitochondrial genes such as COII and COIII in PF forms, indicating that environmental factors contribute to RNA editing regulation during life cycle transitions. However, *in vitro* differentiation conditions mimicking cold shock yielded only partial editing profiles, highlighting the need for additional factors to achieve complete PF differentiation.

## 10. Discussion

The results of this study suggest that RBP7910 overexpression in monomorphic BF *T. brucei* cells initiates molecular and cellular changes resembling differentiation toward the PF stage.

This transformation, marked by mitochondrial enlargement and enhanced cristae development, indicates that RBP7910 may modulate mitochondrial dynamics and RNA processing, promoting the expression of electron transport chain proteins typically restricted to PF cells. These findings suggest a pivotal role for RBP7910 in mitochondrial remodeling associated with differentiation, consistent with previous observations that RNA-binding proteins influence mitochondrial RNA editing [62, 74], crucial for mitochondrial respiratory function in PF *T. brucei*.

The appearance of EP procyclin, a well-known PF marker, in RBP7910-overexpressing cells without cold shock or CCA treatment supports the hypothesis that RBP7910 can independently drive aspects of BF-to-PF differentiation. Unlike cold shock, which induces EP expression only at temperatures above 15°C [82], RBP7910 overexpression alone was sufficient to stimulate EP expression within 48 hours, underscoring its potential as a central regulator of differentiation. Furthermore, the observed synergy between CCA and RBP7910 overexpression, which amplified EP expression beyond levels achieved by CCA alone, suggests a mechanistic overlap between RBP7910 activity and CCA-induced signaling pathways. This synergy implies that RBP7910 may operate along a pathway parallel to or intersecting with CCA-induced differentiation, possibly enhancing the transcriptional or post-transcriptional regulation of key mitochondrial and cell cycle proteins.

A noteworthy finding is the interaction between cold shock and RBP7910 overexpression. While cold shock alone did not induce EP expression, it enhanced EP induction in RBP7910-overexpressing cells. However, an unexpected inhibitory effect occurred when cold shock was applied simultaneously with the onset of RBP7910 overexpression. This suggests a possible early-phase competition or inhibitory cross-talk between RBP7910-mediated processes and pathways activated by cold shock, highlighting the need for further investigation into the timing and molecular dynamics governing EP expression. This inhibition may involve a specific feedback mechanism that remains to be fully elucidated.

The successful expression of EP procyclin and tagged RBP7910 only in tetracycline-induced cells confirms that the observed differentiation effects are due to RBP7910 overexpression. Collectively, these findings underscore RBP7910 as a novel regulatory factor in *T. brucei* differentiation, with the potential to bypass traditional differentiation stimuli like CCA or cold shock. This highlights the therapeutic relevance of targeting RNA-binding proteins to regulate mitochondrial functions and cellular differentiation in trypanosomatid protozoa.

This study provides an in-depth analysis of RBP7910's protein-protein interactions in the BF stage of *T. brucei*, revealing both RNA-dependent and RNA-independent partners with potential roles in BF-to-PF differentiation. IP experiments with V5-tagged RBP7910, followed by RNase A treatment, successfully distinguished direct protein interactions from RNA-mediated ones, advancing our understanding of RBP7910's complex interactome. The RNA-independent interactions, preserved post-RNase treatment, suggest stable, direct binding partners that may

contribute to RBP7910's structural or regulatory functions within the mitochondria, independent of RNA scaffolding.

MS profiling categorized approximately 100 RBP7910-associated proteins in BF cells, complementing previous findings on RBP7910 interactors in PF *T. brucei* [76], and providing a comparative framework for assessing stage-specific roles of this RNA-binding protein. The identification of distinct protein partners in BF cells, many involved in mitochondrial function or RNA processing, underscores RBP7910's dynamic role in mitochondrial RNA biology and stage-specific gene expression in *T. brucei*.

A PPI network constructed in Cytoscape visually categorized RBP7910's interactions, illustrating the complex interplay between RNA-dependent and RNA-independent partners, as well as their relative abundance and functional diversity.

The selective interaction of RBP7910 with specific protein partners in BF and PF stages emphasizes its regulatory flexibility in response to differentiation cues. The RNA-independent interactors in BF cells suggest that RBP7910 may directly engage mitochondrial proteins to maintain BF-specific mitochondrial function. In contrast, the RNA-dependent interactions in PF cells align with increased RNA-editing complex formation, supporting the bioenergetic needs of PF cells.

In summary, these findings broaden our understanding of how RBP7910 mediates stage-specific mitochondrial processes in *T. brucei*. They also highlight the potential of targeting RBP7910 or

its interacting partners to disrupt mitochondrial function in pathogenic trypanosomatids selectively. Further investigation of these interactions across life stages may illuminate new therapeutic avenues targeting RNA-binding proteins essential for *T. brucei* differentiation and survival.

Additionally, this study reveals critical insights into the adaptive mechanisms of mitochondrial RNA processing across parasite life stages, particularly during the BF to PF differentiation. The findings underscore the intricate network of environmental cues, protein complexes, and post-transcriptional modifications that collectively drive stage-specific RNA editing and processing, enabling *T. brucei* to transition between mammalian and insect hosts.

Our analysis of editosome protein abundance profiles during the SS to PF differentiation highlights a significant reshaping of RNA editing machinery. Specifically, proteins such as RBP7910 are upregulated during this transition, supporting the role of specific RNA-processing proteins in initiating mitochondrial RNA editing required for PF metabolic needs and the BF-to-PF transition.

Proteins upregulated both during the BF-to-PF transition and the PF stage, such as KREPA3 and KREH2, could function as dual-purpose regulatory proteins, consistently upregulated through SS and PF stages to support both differentiation and PF growth.

PF-specific proteins, like KRET2 and MEAT1, are upregulated solely in PF stage, correlating with adaptations for oxidative phosphorylation, suggesting a tailored mitochondrial RNA

processing pathway that supports the respiratory demands of PF *T. brucei* in the insect vector environment. This stage-specific regulation aligns with environmental responses to cold shock and glucose restriction, both of which influence mitochondrial gene expression, highlighting the organism's ability to adjust RNA editing in response to host-derived cues. Downregulated proteins, such as KREPB4, exhibited reduced abundance and may act as checkpoint regulators to modulate differentiation.

An important question arises: what drives the distinct expression patterns of editosome proteins at various differentiation stages? Evidence of synchronized initiation of SS trypanosomes into differentiation and cell cycle pathways [83], suggests a possible link between protein expression changes and cell cycle phases. For instance, early downregulation of KREPB4 and RESC12 at 2 hours coincides with the cell's perception of differentiation signals and surface coat alterations, implying that proteins like KREPB4, which is downregulated at 2 hours, may inhibit the editing process—a control lifted upon signal reception SS cells re-entering the cell cycle.

In contrast, KREPA3, another RECC component, shows an opposing expression pattern, hinting at a counter-regulatory function to KREPB4. RESC19 is particularly intriguing, with consistent upregulation from 4 to 48 hours, suggesting a more general regulatory role across differentiation. Meanwhile, the helicase KH2F1 downregulates at 6 hours, preceding the S-phase between 8-12 hours.

Further complexity emerges as KREPA3, RESC9, and KREH1 are upregulated at 12 hours, aligning with S phase completion and G2 entry. This prompts questions about potential links

between editosome proteins, RNA editing, and cell proliferation. This model provides a framework for understanding how RNA editing machinery adapts to the parasite's metabolic shifts. Certain proteins may initiate the editing process by recruiting gRNA and binding to pre-edited mRNA, while others enhance editing efficiency or stabilize edited RNA, ensuring efficient mitochondrial function at each life stage. These insights pave the way for experimental validation of these proposed roles and interactions.

Our analysis of translational efficiency across *T. brucei* life stages reveals how the protozoan fine-tune protein production to meet the demands of its unique life cycle. Notably, translational efficiency does not directly correlate with RNA stability, suggesting control mechanisms beyond traditional RNA degradation pathways. RESC complex members, including RESC16 (PAMC2), TBRGG2, and RESC14 (MRB7260), exhibit increased translational efficiency during the PF stage compared to BF, likely reflecting heightened mitochondrial RNA editing needs in PF to support gRNA-mRNA interactions crucial for insect vector survival.

In contrast, proteins like KREPB9, KREPB5, and the auxiliary factor KREAP1 show reduced translational efficiency in PF, indicating a downscaling of their roles in line with stage-specific demands. This modulation of translational efficiency across protein complexes underscores *T. brucei*'s adaptability, aligning protein synthesis rates with mitochondrial needs.

The regulatory landscape for editosome proteins extends beyond translational efficiency, with RBPs potentially playing a critical role in differentiation. Analysis of RBPs in *T. brucei brucei*

highlighted stage-specific expression patterns with potential regulatory functions. DRBD6A, an RBP with a known binding motif (CAUa/uGU), shows expression changes beginning at 12 hours and continuing into PF, suggesting a role in RNA processing during differentiation. This motif within the UTRs of select editosome proteins—including KREN1, KREPA5, KREPB7, and MPSS3, implies DRBD6A may selectively modulate these transcripts, influencing RNA editing in response to differentiation cues.

Protein phosphorylation also emerges as a significant regulatory mechanism in *T. brucei*, affecting protein function, stability, and localization. Phosphoproteomics data reveal consistent phosphorylation patterns across BF and PF stages, with limited stage exclusivity, indicating stable phosphorylation for editosome proteins. However, the substantial upregulation of phosphorylation in KMRP1 during PF suggests phosphorylation's role in fine-tuning RNA-protein interactions necessary for RNA editing, inviting exploration of other post-translational modifications (PTMs) as stage-specific regulators, especially those interacting with RBPs to modulate editosome functions in alignment with life-cycle demands.

Finally, transcriptomic analyses underline mitochondrial RNA editing's adaptability to environmental stimuli, tuning mitochondrial function to host-vector transitions. Increased editing of cytochrome mRNAs, such as COII and CYb, during differentiation indicates a regulatory mechanism tailored to PF mitochondrial demands. Environmental factors like cold shock and glucose restriction further modulate mitochondrial gene expression, partly mimicking *in vivo* differentiation signals. These editing profiles highlight the complexity of *T. brucei*'s adaptation

strategies, suggesting an interplay between RNA editing and environmental cues that fine-tune mitochondrial functionality across life stages.

## 11. Conclusion and summary

This study significantly advances our understanding of the role of RNA-binding protein RBP7910 in the differentiation of *T. brucei* from its BF to the PF. The findings underscore that RBP7910 overexpression alone induces molecular and cellular changes characteristic of PF differentiation, most notably by promoting mitochondrial enlargement and enhanced cristae development as well as EP procyclin surface coat expression. This remodeling suggests that RBP7910 supports mitochondrial dynamics and RNA processing crucial for the expression of PF-specific ETC proteins, thus facilitating the organism's adaptation to the oxidative metabolic requirements in the insect vector environment.

A remarkable observation is the spontaneous expression of EP procyclin, a well-known PF marker, in RBP7910-overexpressing cells. Unlike environmental stimuli like cold shock, which require specific temperature conditions, RBP7910 independently triggers EP procyclin expression. This suggests a potential intrinsic pathway for differentiation initiated by RBP7910 that operates either parallel to or in synergy with cold shock or chemical agents like cis-aconitate. When combined with CCA, RBP7910 overexpression amplifies EP expression levels, suggesting a mechanistic overlap in transcriptional or post-transcriptional regulation pathways that control mitochondrial and cell cycle proteins during differentiation. However, an inhibitory effect observed when cold shock coincides with RBP7910 overexpression highlights a need for further studies into potential feedback mechanisms and pathway interactions that regulate EP expression and mitochondrial function.

PPI profiling in RBP7910-overexpressing BF cells offers insights into its regulatory role within mitochondria. This study, using V5-tagged RBP7910 and RNase A treatment, identified both RNA-dependent and RNA-independent interactions. RNA-independent partners indicate stable interactions, potentially contributing to mitochondrial structure or function independent of RNA scaffolding. MS data revealed RBP7910-associated proteins in BF cells, many of which play roles in mitochondrial function or RNA processing. This interactome expands our understanding of the dynamic regulation of mitochondrial RNA biology across life stages in *T. brucei*.

Further, a constructed PPI network visually categorizes these interactions, highlighting the diversity of RBP7910's regulatory flexibility in response to differentiation cues. The RNA-independent interactions in BF cells may emphasize RBP7910's role in supporting BF-specific mitochondrial functions, while RNA-dependent interactions in PF cells align with the energy-intensive requirements of the insect stage.

Our analysis of editosome protein abundance during the BF-to-PF differentiation stage highlights the upregulation of specific proteins, such as KREPA3 and KREH2, which may serve dual regulatory roles supporting both differentiation and PF growth. The stage-specific profiles of editosome components like KRET2, exclusively upregulated in the PF stage, underscore a tailored mitochondrial RNA processing pathway that meets the metabolic demands of PF cells. Downregulated proteins, including KREPB4, potentially act as checkpoints to regulate differentiation, while the upregulation of other components corresponds with S-phase and cell cycle transitions, suggesting possible links between RNA editing machinery and cell proliferation.

Additionally, this study delves into translational efficiency modulation across life stages, revealing how *T. brucei* aligns protein production with mitochondrial needs. Notably, proteins like TBRGG2 show heightened translational efficiency during PF, reflecting increased RNA-editing demands for the PF's oxidative environment. This targeted translation of specific proteins points to an adaptive strategy that balances mitochondrial function with host-vector transitions.

The role of RBPs as regulators of editosome components emerges prominently in the differentiation process. DRBD6A, identified as having a potential regulatory motif in UTRs of select editosome proteins, displays stage-specific expression changes and may selectively bind and influence transcripts critical for RNA editing. Protein phosphorylation, particularly upregulated in PF-specific proteins like KMRP1, provides an additional layer of regulation, suggesting that PTMs modulate RNA-editing functions in response to differentiation demands.

This research also highlights mitochondrial RNA editing's adaptability to environmental cues, with increased editing of mitochondrial genes such as cytochrome mRNAs COII and CYb during differentiation. This gene-specific editing response highlights an intricate regulatory mechanism that enables *T. brucei* to meet the respiratory demands of the PF stage. Environmental cues like cold shock and glucose restriction replicate aspects of differentiation signals, underscoring how *T. brucei* fine-tunes its mitochondrial function to align with host-derived signals in its life cycle.

In conclusion, RBP7910 stands out as a critical factor in the BF-to-PF differentiation process in *T. brucei*, both as an intrinsic driver and a synergistic enhancer of established differentiation

signals. This study's findings contribute to a broader understanding of how *T. brucei* utilizes stage-specific RNA processing and protein interactions to thrive in diverse host environments. Targeting RBP7910 and its associated pathways holds potential for therapeutic interventions aimed at disrupting the differentiation and survival mechanisms of pathogenic trypanosomatids. This research paves the way for future experimental validation of proposed roles and interactions, advancing our grasp of trypanosomatid biology and the development of anti-parasitic strategies.

## 12.Future directions

This study has focused on monomorphic cell lines representing the two main life stages of *T. brucei*, BF and PF, to explore the effects of RBP7910 overexpression on differentiation and identify the key protein interactions associated with this process. However, monomorphic cell lines provide a simplified model to examine core components of *T. brucei*'s differentiation machinery, they may not fully capture the nuanced shifts in protein abundance and interactions during natural life cycle transition.

In contrast, pleomorphic cell lines, which retain the full differentiation potential from the slender BF to the stumpy form and eventually to the PF, display marked changes in the abundance of several editosome-associated proteins, including RBP7910, at specific transition points [71]. Given that only the SS form can differentiate into the PF, we hypothesize that pleomorphic cell lines capable of synchronized BF-to-PF differentiation offer a more representative system. This model would enable observation of dynamic interactions within the editosome and the mitochondrial RNA-processing proteome at multiple time points, allowing a more detailed analysis of differential RNA editing activity and regulatory mechanisms essential for *T. brucei*'s adaptation to environmental changes between hosts.

We anticipate that these findings will shed new light on the spatial and temporal dynamics of mitochondrial RNA processing pathways regulating mitochondrial gene expression across the parasite's different life stages, enhancing our understanding of the dynamic interactions involving RESC proteins and RBP7910 that drive the assembly and remodeling of mitochondrial RNA processing machinery.

### 13. References

1. Cardo, L.J., *Leishmania: risk to the blood supply*. Transfusion, 2006. **46**(9): p. 1641-1645.
2. Özcan, D., D. Seçkin, A.M. Allahverdiyev, P.J. Weina, H. Aydin, F. Özçay, and M. Haberal, *Liver transplant recipient with concomitant cutaneous and visceral leishmaniasis*. Pediatric transplantation, 2007. **11**(2): p. 228-232.
3. Bern, C., S.P. Montgomery, L. Katz, S. Caglioti, and S.L. Stramer, *Chagas disease and the US blood supply*. Current opinion in infectious diseases, 2008. **21**(5): p. 476-482.
4. Riera, C., R. Fisa, P. López-Chejade, T. Serra, E. Girona, M. Jiménez, J. Muncunill, M. Sedeño, M. Mascaró, and M. Udina, *Asymptomatic infection by Leishmania infantum in blood donors from the Balearic Islands (Spain)*. Transfusion, 2008. **48**(7): p. 1383-1389.
5. Kun, H., A. Moore, L. Mascola, S. Frank, L. Gena, B. Kubak, S. Radhakrishna, D. Leiby, R. Herron, and T. Mone, *Transmission of Trypanosoma cruzi by heart transplantation*. Clinical Infectious Diseases, 2009. **48**(11): p. 1534-1540.
6. Kikwai, C. and M. Ngeiywa, *Review on the Socio-Economic Impacts of Trypanosomiasis*. 2022.
7. Matthews, K.R., *The developmental cell biology of Trypanosoma brucei*. Journal of cell science, 2005. **118**(2): p. 283-290.
8. Erben, E.D., *High-throughput methods for dissection of trypanosome gene regulatory networks*. Current Genomics, 2018. **19**(2): p. 78-86.
9. Najafabadi, H.S., Z. Lu, C. MacPherson, V. Mehta, V. Adoue, T. Pastinen, and R. Salavati, *Global identification of conserved post-transcriptional regulatory programs in trypanosomatids*. Nucleic acids research, 2013. **41**(18): p. 8591-8600.
10. Roditi, I., M. Carrington, and M. Turner, *Expression of a polypeptide containing a dipeptide repeat is confined to the insect stage of Trypanosoma brucei*. Nature, 1987. **325**(6101): p. 272-274.
11. Mowatt, M.R. and C.E. Clayton, *Developmental regulation of a novel repetitive protein of Trypanosoma brucei*. Molecular and cellular biology, 1987. **7**(8): p. 2838-2844.
12. Mowatt, M.R., G.S. Wisdom, and C.E. Clayton, *Variation of tandem repeats in the developmentally regulated procyclic acidic repetitive proteins of Trypanosoma brucei*. Molecular and cellular biology, 1989. **9**(3): p. 1332-1335.
13. Mowatt, M.R. and C.E. Clayton, *Polymorphism in the procyclic acidic repetitive protein gene family of Trypanosoma brucei*. Molecular and cellular biology, 1988. **8**(10): p. 4055-4062.
14. Mehlert, A., A. Treumann, and M.A. Ferguson, *Trypanosoma brucei GPEET-PARP is phosphorylated on six out of seven threonine residues*. Molecular and biochemical parasitology, 1999. **98**(2): p. 291-296.
15. Vassella, E., J. Van Den Abbeele, P. Bütikofer, C.K. Renggli, A. Furger, R. Brun, and I. Roditi, *A major surface glycoprotein of Trypanosoma brucei is expressed transiently during development and can be regulated post-transcriptionally by glycerol or hypoxia*. Genes & development, 2000. **14**(5): p. 615-626.

16. Vickerman, K., L. Tetley, K.A. Hendry, and C.M.R. Turner, *Biology of African trypanosomes in the tsetse fly*. *Biology of the Cell*, 1988. **64**(2): p. 109-119.
17. Bringaud, F., L. Rivière, and V. Coustou, *Energy metabolism of trypanosomatids: adaptation to available carbon sources*. *Molecular and biochemical parasitology*, 2006. **149**(1): p. 1-9.
18. Seed, J.R. and M.A. Wenck, *Role of the long slender to short stumpy transition in the life cycle of the African trypanosomes*. *Kinetoplastid Biology and Disease*, 2003. **2**: p. 1-8.
19. MacGregor, P., B. Szöör, N.J. Savill, and K.R. Matthews, *Trypanosomal immune evasion, chronicity and transmission: an elegant balancing act*. *Nature Reviews Microbiology*, 2012. **10**(6): p. 431-438.
20. Zimmermann, H., I. Subota, C. Batram, S. Kramer, C.J. Janzen, N.G. Jones, and M. Engstler, *A quorum sensing-independent path to stumpy development in Trypanosoma brucei*. *PLOS pathogens*, 2017. **13**(4): p. e1006324.
21. Ziegelbauer, K., M. Quinten, H. Schwarz, T.W. Pearson, and P. Overath, *Synchronous differentiation of Trypanosoma brucei from bloodstream to procyclic forms in vitro*. *European journal of biochemistry*, 1990. **192**(2): p. 373-378.
22. Read, L.K., J. Lukeš, and H. Hashimi, *Trypanosome RNA editing: the complexity of getting U in and taking U out*. *Wiley Interdisciplinary Reviews: RNA*, 2016. **7**(1): p. 33-51.
23. Aphasizheva, I., J. Alfonzo, J. Carnes, I. Cestari, J. Cruz-Reyes, H.U. Göringer, S. Hajduk, J. Lukeš, S. Madison-Antenucci, and D.A. Maslov, *Lexis and grammar of mitochondrial RNA processing in trypanosomes*. *Trends in parasitology*, 2020. **36**(4): p. 337-355.
24. Aphasizheva, I., L. Zhang, X. Wang, R.M. Kaake, L. Huang, S. Monti, and R. Aphasizhev, *RNA binding and core complexes constitute the U-insertion/deletion editosome*. *Molecular and cellular biology*, 2014. **34**(23): p. 4329-4342.
25. Blum, B., N. Bakalara, and L. Simpson, *A model for RNA editing in kinetoplastid mitochondria*. 1991.
26. Lukeš, J., H. Hashimi, and A. Zíková, *Unexplained complexity of the mitochondrial genome and transcriptome in kinetoplastid flagellates*. *Current genetics*, 2005. **48**: p. 277-299.
27. Koslowsky, D.J., L. Reifur, L. Yu, and W. Chen, *Evidence for U-tail stabilization of gRNA/mRNA interactions in kinetoplastid RNA editing*. *RNA biology*, 2004. **1**(1): p. 27-33.
28. Salavati, R., H. Moshiri, S. Kala, and H.S. Najafabadi, *Inhibitors of RNA editing as potential chemotherapeutics against trypanosomatid pathogens*. *International Journal for Parasitology: Drugs and Drug Resistance*, 2012. **2**: p. 36-46.
29. Maslov, D.A. and L. Simpson, *The polarity of editing within a multiple gRNA-mediated domain is due to formation of anchors for upstream gRNAs by downstream editing*. *Cell*, 1992. **70**(3): p. 459-467.
30. Li, F., J. Herrera, S. Zhou, D.A. Maslov, and L. Simpson, *Trypanosome REH1 is an RNA helicase involved with the 3'-5' polarity of multiple gRNA-guided uridine insertion/deletion RNA editing*. *Proceedings of the National Academy of Sciences*, 2011. **108**(9): p. 3542-3547.
31. Madison-Antenucci, S., J. Grams, and S.L. Hajduk, *Editing machines: the complexities of trypanosome RNA editing*. *Cell*, 2002. **108**(4): p. 435-438.

32. Horváth, A., E. Horáková, P. Dunajčíková, Z. Verner, E. Pravdová, I. Šlapetová, L.u. Cuninková, and J. Lukeš, *Downregulation of the nuclear-encoded subunits of the complexes III and IV disrupts their respective complexes but not complex I in procyclic Trypanosoma brucei*. Molecular microbiology, 2005. **58**(1): p. 116-130.
33. Schnauffer, A., G.D. Clark-Walker, A.G. Steinberg, and K. Stuart, *The F1-ATP synthase complex in bloodstream stage trypanosomes has an unusual and essential function*. The EMBO journal, 2005. **24**(23): p. 4029-4040.
34. Schnauffer, A., A.K. Panigrahi, B. Panicucci, R.P. Igo Jr, R. Salavati, and K. Stuart, *An RNA ligase essential for RNA editing and survival of the bloodstream form of Trypanosoma brucei*. Science, 2001. **291**(5511): p. 2159-2162.
35. Carnes, J., J.R. Trotter, N.L. Ernst, A. Steinberg, and K. Stuart, *An essential RNase III insertion editing endonuclease in Trypanosoma brucei*. Proceedings of the National Academy of Sciences, 2005. **102**(46): p. 16614-16619.
36. *Generation of membrane potential in trypanosomes*. 2011, Schnauffer lab.
37. Gazestani, V.H., M. Hampton, A.K. Shaw, R. Salavati, and S.L. Zimmer, *Tail characteristics of Trypanosoma brucei mitochondrial transcripts are developmentally altered in a transcript-specific manner*. International Journal for Parasitology, 2018. **48**(2): p. 179-189.
38. McDermott, S.M., J. Carnes, and K. Stuart, *Identification by random mutagenesis of functional domains in KREPB5 that differentially affect RNA editing between life cycle stages of Trypanosoma brucei*. Molecular and cellular biology, 2015.
39. Guo, X., N.L. Ernst, and K.D. Stuart, *The KREPA3 zinc finger motifs and OB-fold domain are essential for RNA editing and survival of Trypanosoma brucei*. Molecular and cellular biology, 2008.
40. Koslowsky, D.J., G.R. Riley, J.E. Feagin, and K. Stuart, *Guide RNAs for transcripts with developmentally regulated RNA editing are present in both life cycle stages of Trypanosoma brucei*. Molecular and cellular biology, 1992. **12**(5): p. 2043-2049.
41. Riley, G.R., P.J. Myler, and K. Stuart, *Quantitation of RNA editing substrates, products and potential intermediates: implications for developmental regulation*. Nucleic acids research, 1995. **23**(4): p. 708-712.
42. Reifur, L., L.E. Yu, J. Cruz-Reyes, M. Vanhartesvelt, and D.J. Koslowsky, *The impact of mRNA structure on guide RNA targeting in kinetoplastid RNA editing*. PloS one, 2010. **5**(8): p. e12235.
43. Madina, B.R., V. Kumar, R. Metz, B.H. Mooers, R. Bundschuh, and J. Cruz-Reyes, *Native mitochondrial RNA-binding complexes in kinetoplastid RNA editing differ in guide RNA composition*. Rna, 2014. **20**(7): p. 1142-1152.
44. AMMERMAN, M.L., H. HASHIMI, L. NOVOTNA, Z. ČIČŮVA, S.M. MCEVOY, J. LUKEŠ, and L.K. READ, *MRB3010 is a core component of the MRB1 complex that facilitates an early step of the kinetoplastid RNA editing process*. RNA, 2011. **17**: p. 00-00.
45. Hashimi, H., A. Zikova, A.K. Panigrahi, K.D. Stuart, and J. Lukes, *TbRGG1, an essential protein involved in kinetoplastid RNA metabolism that is associated with a novel multiprotein complex*. RNA, 2008. **14**(5): p. 970-80.

46. Weng, J., I. Aphasizheva, R.D. Etheridge, L. Huang, X. Wang, A.M. Falick, and R. Aphasizhev, *Guide RNA-binding complex from mitochondria of trypanosomatids*. Molecular cell, 2008. **32**(2): p. 198-209.
47. Panigrahi, A.K., A. Zikova, R.A. Dalley, N. Acestor, Y. Ogata, A. Anupama, P.J. Myler, and K.D. Stuart, *Mitochondrial complexes in Trypanosoma brucei: a novel complex and a unique oxidoreductase complex*. Mol Cell Proteomics, 2008. **7**(3): p. 534-45.
48. Hashimi, H., Z. Čičová, L. Novotná, Y.-Z. Wen, and J. Lukeš, *Kinetoplastid guide RNA biogenesis is dependent on subunits of the mitochondrial RNA binding complex 1 and mitochondrial RNA polymerase*. Rna, 2009. **15**(4): p. 588-599.
49. Ammerman, M.L., D.L. Tomasello, D. Faktorová, L. Kafková, H. Hashimi, J. Lukeš, and L.K. Read, *A core MRB1 complex component is indispensable for RNA editing in insect and human infective stages of Trypanosoma brucei*. PLoS one, 2013. **8**(10): p. e78015.
50. Allen, T.E., S. Heidmann, R. Reed, P.J. Myler, H.U. Göringer, and K.D. Stuart, *Association of guide RNA binding protein gBP21 with active RNA editing complexes in Trypanosoma brucei*. Molecular and cellular biology, 1998. **18**(10): p. 6014-6022.
51. Osato, D., K. Rogers, Q. Guo, F. Li, G. Richmond, F. Klug, and L. Simpson, *Uridine insertion/deletion RNA editing in trypanosomatid mitochondria: In search of the editosome*. RNA, 2009. **15**(7): p. 1338-44.
52. Aphasizhev, R., I. Aphasizheva, R.E. Nelson, and L. Simpson, *A 100-kD complex of two RNA-binding proteins from mitochondria of Leishmania tarentolae catalyzes RNA annealing and interacts with several RNA editing components*. Rna, 2003. **9**(1): p. 62-76.
53. Gerstberger, S., M. Hafner, and T. Tuschl, *A census of human RNA-binding proteins*. Nature Reviews Genetics, 2014. **15**(12): p. 829-845.
54. Clayton, C., *Gene expression in Kinetoplastids*. Current opinion in microbiology, 2016. **32**: p. 46-51.
55. Clayton, C. and M. Shapira, *Post-transcriptional regulation of gene expression in trypanosomes and leishmanias*. Mol Biochem Parasitol, 2007. **156**(2): p. 93-101.
56. Haile, S. and B. Papadopoulou, *Developmental regulation of gene expression in trypanosomatid parasitic protozoa*. Current opinion in microbiology, 2007. **10**(6): p. 569-577.
57. Begolo, D., I.M. Vincent, F. Giordani, I. Pöhner, M.J. Witty, T.G. Rowan, Z. Bengaly, K. Gillingwater, Y. Freund, and R.C. Wade, *The trypanocidal benzoxaborole AN7973 inhibits trypanosome mRNA processing*. PLoS pathogens, 2018. **14**(9): p. e1007315.
58. Wall, R.J., E. Rico, I. Lukac, F. Zuccotto, S. Elg, I.H. Gilbert, Y. Freund, M.R. Alley, M.C. Field, and S. Wyllie, *Clinical and veterinary trypanocidal benzoxaboroles target CPSF3*. Proceedings of the National Academy of Sciences, 2018. **115**(38): p. 9616-9621.
59. Kolev, N.G., E. Ullu, and C. Tschudi, *The emerging role of RNA-binding proteins in the life cycle of Trypanosoma brucei*. Cellular microbiology, 2014. **16**(4): p. 482-489.
60. Clayton, C., *Regulation of gene expression in trypanosomatids*. 2019.
61. Wurst, M., B. Seliger, B.A. Jha, C. Klein, R. Queiroz, and C. Clayton, *Expression of the RNA recognition motif protein RBP10 promotes a bloodstream-form transcript pattern in Trypanosoma brucei*. Molecular microbiology, 2012. **83**(5): p. 1048-1063.

62. Kolev, N.G., K. Ramey-Butler, G.A. Cross, E. Ullu, and C. Tschudi, *Developmental progression to infectivity in Trypanosoma brucei triggered by an RNA-binding protein*. Science, 2012. **338**(6112): p. 1352-1353.
63. Toh, J.Y., A. Nkouawa, S.R. Sánchez, H. Shi, N.G. Kolev, and C. Tschudi, *Identification of positive and negative regulators in the stepwise developmental progression towards infectivity in Trypanosoma brucei*. Scientific reports, 2021. **11**(1): p. 5755.
64. Gazestani, V.H., N. Nikpour, V. Mehta, H.S. Najafabadi, H. Moshiri, A. Jardim, and R. Salavati, *A protein complex map of Trypanosoma brucei*. PLoS neglected tropical diseases, 2016. **10**(3): p. e0004533.
65. Nikpour, N. and R. Salavati, *The RNA binding activity of the first identified trypanosome protein with Z-DNA-binding domains*. Scientific Reports, 2019. **9**(1): p. 5904.
66. Ehlert, C., N. Poorinmohammad, S. Mohammedi, L. Zhang, and R. Salavati, *Structure–Function Analysis of RBP7910: An Edosome Z-Binding Protein in Trypanosomatids*. Molecules, 2023. **28**(19): p. 6963.
67. Brown, B.A., K. Lowenhaupt, C.M. Wilbert, E.B. Hanlon, and A. Rich, *The Z $\alpha$  domain of the editing enzyme dsRNA adenosine deaminase binds left-handed Z-RNA as well as Z-DNA*. Proceedings of the National Academy of Sciences, 2000. **97**(25): p. 13532-13536.
68. Sement, F.M., T. Suematsu, L. Zhang, T. Yu, L. Huang, I. Aphasizheva, and R. Aphasizhev, *Transcription initiation defines kinetoplast RNA boundaries*. Proceedings of the National Academy of Sciences, 2018. **115**(44): p. E10323-E10332.
69. Butter, F., F. Bucerius, M. Michel, Z. Cicova, M. Mann, and C.J. Janzen, *Comparative proteomics of two life cycle stages of stable isotope-labeled Trypanosoma brucei reveals novel components of the parasite's host adaptation machinery*. Molecular & Cellular Proteomics, 2013. **12**(1): p. 172-179.
70. Zamani, H., N. Poorinmohammad, A. Azimi, and R. Salavati, *From a bimodal to a multi-stage view on trypanosomes' differential RNA editing*. Trends in Parasitology, 2024.
71. Dejung, M., I. Subota, F. Bucerius, G. Dindar, A. Freiwald, M. Engstler, M. Boshart, F. Butter, and C.J. Janzen, *Quantitative proteomics uncovers novel factors involved in developmental differentiation of Trypanosoma brucei*. PLoS pathogens, 2016. **12**(2): p. e1005439.
72. Smith Jr, J.T., B. Tylec, A. Naguleswaran, I. Roditi, and L.K. Read, *Developmental dynamics of mitochondrial mRNA abundance and editing reveal roles for temperature and the differentiation-repressive kinase RDK1 in cytochrome oxidase subunit II mRNA editing*. Mbio, 2023. **14**(5): p. e01854-23.
73. Moretti, N.S., I. Cestari, A. Anupama, K. Stuart, and S. Schenkman, *Comparative proteomic analysis of lysine acetylation in trypanosomes*. Journal of proteome research, 2018. **17**(1): p. 374-385.
74. Mugo, E. and C. Clayton, *Expression of the RNA-binding protein RBP10 promotes the bloodstream-form differentiation state in Trypanosoma brucei*. PLoS pathogens, 2017. **13**(8): p. e1006560.
75. Briggs, E.M., F. Rojas, R. McCulloch, K.R. Matthews, and T.D. Otto, *Single-cell transcriptomic analysis of bloodstream Trypanosoma brucei reconstructs cell cycle progression and developmental quorum sensing*. Nat Commun, 2021. **12**(1): p. 5268.
76. Ramamurthy, N., *The biological role of the RBP7910 Z-binding*

*protein in the mitochondrial mRNA processing of Trypanosoma brucei*, in *Parasitology Institute*. 2020, McGill.

77. Alvarez-Jarreta, J., B. Amos, C. Aurrecochea, S. Bah, M. Barba, A. Barreto, E.Y. Basenko, R. Belnap, A. Blevins, and U. Böhme, *VEuPathDB: the eukaryotic pathogen, vector and host bioinformatics resource center in 2023*. *Nucleic acids research*, 2024. **52**(D1): p. D808-D816.
78. Vasquez, J.-J., C.-C. Hon, J.T. Vanselow, A. Schlosser, and T.N. Siegel, *Comparative ribosome profiling reveals extensive translational complexity in different Trypanosoma brucei life cycle stages*. *Nucleic acids research*, 2014. **42**(6): p. 3623-3637.
79. Alsford, S., D.J. Turner, S.O. Obado, A. Sanchez-Flores, L. Glover, M. Berriman, C. Hertz-Fowler, and D. Horn, *High-throughput phenotyping using parallel sequencing of RNA interference targets in the African trypanosome*. *Genome research*, 2011. **21**(6): p. 915-924.
80. Urbaniak, M.D., D.M. Martin, and M.A. Ferguson, *Global quantitative SILAC phosphoproteomics reveals differential phosphorylation is widespread between the procyclic and bloodstream form lifecycle stages of Trypanosoma brucei*. *Journal of proteome research*, 2013. **12**(5): p. 2233-2244.
81. Urbaniak, M.D., D.M.A. Martin, and M.A.J. Ferguson, *Global Quantitative SILAC Phosphoproteomics Reveals Differential Phosphorylation Is Widespread between the Procyclic and Bloodstream Form Lifecycle Stages of Trypanosoma brucei*. *Journal of Proteome Research*, 2013. **12**(5): p. 2233-2244.
82. Engstler, M. and M. Boshart, *Cold shock and regulation of surface protein trafficking convey sensitization to inducers of stage differentiation in Trypanosoma brucei*. *Genes & development*, 2004. **18**(22): p. 2798-2811.
83. Matthews, K.R. and K. Gull, *Evidence for an interplay between cell cycle progression and the initiation of differentiation between life cycle forms of African trypanosomes*. *The Journal of cell biology*, 1994. **125**(5): p. 1147-1156.

## 14. Appendix

Appendix 1- The comprehensive MS dataset is presented in the table below:

Accession Number	MW	Tet-	Tet-	Tet+ RNase+	Tet+ RNase-	Tet+ RNase-	Tet+ RNase+	Tet+ RNase-
Q387U4	377 kDa	0	1	103	109	13	19	39
Q581U8	75 kDa	0	0	31	28	0	2	0
Q581Q1 (+1)	49 kDa	0	0	31	6	0	5	0
Q38CC3	197 kDa	0	0	26	30	0	0	0
Q582N2	42 kDa	0	0	20	7	0	1	0
Q386F2	31 kDa	0	0	18	8	0	2	0
Q386Y0	90 kDa	0	0	18	13	0	0	0
Q389P1	81 kDa	0	0	17	26	1	0	0
Q38EP5	30 kDa	0	0	16	16	1	3	0
Q57WF2	67 kDa	0	0	16	13	0	0	0
Q586A8	94 kDa	0	0	16	11	0	0	0
Q38C20	66 kDa	0	0	16	1	0	0	0
Q57V54 (+1)	25 kDa	0	0	15	8	0	6	0
Q384N5	31 kDa	0	0	15	18	0	0	2
Q38BY1	85 kDa	0	0	15	13	0	0	0
Q57W56	28 kDa	0	0	15	2	0	4	0
Q57V35 (+1)	29 kDa	0	0	15	3	0	1	0
Q57VM1	31 kDa	0	0	15	0	0	2	0
Q57ZI7	29 kDa	2	0	14	8	4	3	0
Q38CJ3	66 kDa	0	0	14	10	0	1	0
Q4GZ30	129 kDa	0	0	13	11	0	0	0
Q38BK6 (+1)	29 kDa	0	0	13	1	0	1	0
Q389K1	21 kDa	0	0	13	0	0	0	0
Q38CY8	35 kDa	0	0	12	0	0	3	0
Q38CW9	15 kDa	0	0	11	4	0	1	0
Q584G9	17 kDa	0	0	11	1	0	2	0
Q583M4	48 kDa	0	0	10	6	0	0	0
Q381J6	16 kDa	0	0	10	2	0	2	0

Q57ZH1 (+1)	25 kDa	0	0	10	1	0	1	0
Q583T1	21 kDa	0	0	10	1	0	2	0
Q57VP3	22 kDa	0	0	10	2	0	0	0
Q385E9	17 kDa	0	0	10	2	0	0	0
Q4GYQ5	20 kDa	0	0	10	1	0	0	0
Q382C4	21 kDa	0	0	9	5	0	1	0
Q38EC5	25 kDa	0	0	9	5	0	1	0
D7SG81	12 kDa	0	0	9	2	0	2	0
Q38CL9	28 kDa	0	0	9	4	0	2	0
Q382Z8	16 kDa	0	0	9	2	0	1	0
Q386V3	35 kDa	0	0	9	0	0	0	0
Q38EI9	22 kDa	0	0	9	0	0	0	0
Q383E5	75 kDa	0	5	8	3	0	0	2
Q580D8	18 kDa	0	0	8	4	0	1	0
Q383V6 (+1)	19 kDa	0	0	8	2	0	1	0
Q57ZL2	65 kDa	0	0	8	6	0	0	0
Q389I7 (+1)	24 kDa	0	0	8	2	0	2	0
P50885	22 kDa	0	0	8	0	0	0	0
Q383E1	35 kDa	0	0	8	0	0	0	0
Q38EY2	48 kDa	0	0	8	0	0	0	0
Q38D58	11 kDa	0	4	7	5	0	1	0
P86934 (+1)	49 kDa	0	1	7	8	1	0	1
Q388A9	87 kDa	0	0	7	9	0	0	0
Q580S6	78 kDa	0	0	7	7	0	0	0
Q38D25 (+1)	16 kDa	0	0	7	3	0	0	0
Q38FD9	24 kDa	0	0	7	2	0	3	0
Q583K7	19 kDa	0	0	7	5	0	0	0
Q8IFI8	98 kDa	0	0	7	5	0	0	0
Q38DH8	22 kDa	0	0	7	2	0	0	0
Q384J9	13 kDa	0	0	7	0	0	0	0
Q388D3	29 kDa	0	0	7	0	0	0	0
Q385D9	21 kDa	0	0	7	0	0	0	0
Q38B01	191 kDa	0	0	6	15	0	0	0
Q57WZ2	53 kDa	0	0	6	6	0	0	0
Q385T6	19 kDa	0	0	6	4	0	1	0
Q386T4	27 kDa	0	0	6	5	0	0	0

Q389K8	46 kDa	0	0	6	7	0	0	0
Q586C2	17 kDa	0	0	6	1	0	0	0
Q387J6	31 kDa	0	0	6	2	0	0	0
Q383I8 (+1)	31 kDa	0	0	6	0	0	1	0
Q585J5	26 kDa	0	0	6	1	0	0	0
Q38BI8 (+1)	12 kDa	0	0	6	0	0	0	0
Q38CD0	22 kDa	0	0	6	0	0	0	0
Q388B0	72 kDa	0	0	5	7	0	0	0
Q38FW8	15 kDa	0	0	5	2	0	0	0
Q38AC1	16 kDa	0	0	5	0	0	0	0
Q38DN9	16 kDa	0	0	5	2	0	1	0
Q381S3	79 kDa	0	0	5	5	0	0	0
Q584X2	15 kDa	0	0	5	5	0	0	0
Q38CY7 (+1)	26 kDa	0	0	5	0	0	1	0
Q57VV0	17 kDa	0	0	5	3	0	0	0
Q38B69	18 kDa	0	0	5	2	0	0	0
Q57YL6	25 kDa	0	0	5	1	0	0	0
Q386L1	10 kDa	0	0	5	1	0	0	0
Q382D5 (+1)	30 kDa	0	0	5	0	0	0	0
Q387Z3	41 kDa	0	0	5	0	0	0	0
Q38BV6	47 kDa	0	0	5	0	0	0	0
Q38CY6	12 kDa	0	0	5	0	0	0	0
Q586G9	83 kDa	0	0	5	0	0	0	0
Q4GYY5	50 kDa	0	2	4	7	0	0	1
Q388B7	91 kDa	0	0	4	16	0	0	0
Q4GYY6	50 kDa	0	0	4	5	0	0	0
D7SGA2	98 kDa	0	0	4	3	0	0	0
Q582R3	73 kDa	0	0	4	7	0	0	0
Q38AZ9	15 kDa	0	0	4	3	0	0	0
Q38B98 (+1)	17 kDa	0	0	4	1	0	0	0
Q38B00	22 kDa	0	0	4	1	0	0	1
Q4FKG9	16 kDa	0	0	4	2	0	0	0
Q38A80	45 kDa	0	0	4	2	0	0	0
Q38CD1	16 kDa	0	0	4	1	0	0	0
Q57U30	11 kDa	0	0	4	0	0	0	0
Q387G2	19 kDa	0	0	4	0	0	0	0
Q57ZR8	40 kDa	0	0	4	0	0	0	0

Q580K6	15 kDa	0	0	4	0	0	0	0
Q385C8	163 kDa	0	0	4	0	0	0	0
Q389U9	255 kDa	0	0	3	3	0	0	10
Q38E94	42 kDa	0	0	3	7	0	0	0
Q381A3	24 kDa	0	0	3	3	0	0	0
Q586R7	50 kDa	0	0	3	3	0	0	0
Q383T7	77 kDa	0	0	3	3	0	0	0
Q38D53 (+1)	24 kDa	0	0	3	0	0	0	0
Q57UJ8	7 kDa	0	0	3	0	0	0	0
Q38EY6	11 kDa	0	0	3	0	0	0	0
Q38DP2	15 kDa	0	0	3	0	0	0	0
Q383N6	64 kDa	0	0	3	0	0	0	0
Q38BE4	94 kDa	0	0	3	0	0	0	0
Q57XL0	51 kDa	0	0	3	0	0	0	0
Q57XX0	13 kDa	0	0	3	0	0	0	0
Q388E8	71 kDa	0	0	3	0	0	0	0
Q38B66 (+1)	19 kDa	0	0	3	0	0	0	0
Q38BR9	10 kDa	0	0	3	0	0	0	0
Q38B42	41 kDa	10	14	2	6	0	1	8
Q38DE9 (+3)	56 kDa	0	1	2	3	0	0	0
Q38AH3	21 kDa	0	0	2	3	0	0	2
Q57UA5	125 kDa	0	0	2	5	0	0	0
Q38AW9	10 kDa	0	0	2	1	0	1	0
Q38AG5	39 kDa	0	0	2	3	0	0	0
Q57XK6	69 kDa	0	0	2	3	0	0	0
Q385B8 (+1)	21 kDa	0	0	2	0	0	1	0
Q383X4	38 kDa	0	0	2	3	0	0	0
Q38B56 (+1)	15 kDa	0	0	2	1	0	0	0
Q585H2	95 kDa	0	0	2	0	0	0	0
Q383S6	8 kDa	0	0	2	0	0	2	0
Q38D86	48 kDa	0	0	2	2	0	0	0
Q388M7	41 kDa	0	0	2	2	0	0	0
Q38BA1	29 kDa	0	0	2	2	0	0	0
Q38DX4	54 kDa	0	0	2	1	0	0	0

Q38DF6 (+1)	83 kDa	0	0	2	0	0	1	0
Q38DH5	40 kDa	0	0	2	1	0	0	0
Q38F76	45 kDa	0	0	2	1	0	0	0
Q388D4	38 kDa	0	0	2	0	0	0	0
Q38AM9	16 kDa	0	0	2	0	0	0	0
Q57Z31	11 kDa	0	0	2	0	0	0	0
Q38B23	48 kDa	0	0	2	0	0	0	0
Q57UA6	104 kDa	0	0	2	0	0	0	0
Q57VZ2	37 kDa	0	0	2	0	0	0	0
Q386P9	51 kDa	0	0	2	0	0	0	0
Q383R3 (+1)	15 kDa	0	0	2	0	0	0	0
Q388I8	38 kDa	0	0	2	0	0	0	0
Q585V4	45 kDa	0	7	1	0	0	0	0
Q586Z5 (+1)	44 kDa	0	5	1	3	0	0	0
Q57Y20	103 kDa	0	0	1	4	0	0	0
Q384Y3	29 kDa	0	0	1	3	0	0	0
Q582R3	?	0	0	1	2	0	0	0
Q57W67	71 kDa	0	3	0	0	0	0	0
Q57YW0	38 kDa	0	2	0	1	0	0	0
Q389N2	46 kDa	0	2	0	0	0	0	0
Q384Q5	71 kDa	0	1	0	0	0	0	3
Q38D54	35 kDa	0	0	0	3	0	0	8
Q38DE8	135 kDa	0	0	0	8	0	0	0
Q57XL7	53 kDa	0	0	0	4	0	0	2
Q389P7	32 kDa	0	0	0	1	0	0	3
Q386H5	103 kDa	0	0	0	5	0	0	0
D7SGA3 (+2)	95 kDa	0	0	0	2	0	0	0
Q586X1	55 kDa	0	0	0	3	0	0	1
Q382N3	17 kDa	0	0	0	2	0	1	0
Q57WL2	103 kDa	0	0	0	3	0	0	0
Q386R7	485 kDa	0	0	0	3	0	0	0
Q387Q3	48 kDa	0	0	0	0	0	0	2
D6XDN4	54 kDa	0	0	0	0	0	0	2

Q382C8	52 kDa	0	0	0	2	0	0	0
Q381B0	55 kDa	0	0	0	2	0	0	0
Q57WZ3	24 kDa	0	0	0	2	0	0	0
Q383L4	100 kDa	0	0	0	2	0	0	0
Q38DH2	18 kDa	0	0	0	2	0	0	0

**Appendix 2- The full list of RBPs alongside their expression profile during BF-to-PF differentiation:**

<b>Not-regulated</b>	<b>Significantly upregulated in the PF</b>	<b>Significantly upregulated during the BF-to-PF differentiation and/or the PF</b>
Tb10.v4.0040	Tb11.02.5380	Tb10.v4.0033
Tb11.02.5120b	Tb11.02.5390	Tb11.v5.0248
Tb11.0290	Tb11.v5.1059	Tb11.v5.0631
Tb11.0390	Tb927.10.13500	Tb11.v5.0730
Tb11.v5.0152	Tb927.10.4560	Tb11.v5.0767
Tb11.v5.0171	Tb927.10.9880	Tb11.v5.0199
Tb11.v5.0179	Tb927.11.11360	Tb11.v5.0684
Tb11.v5.0246	Tb927.11.16280	Tb11.v5.1053
Tb11.v5.0252	Tb927.11.3590	Tb927.11.3000
Tb11.v5.0291	Tb927.11.4050	Tb927.3.3960
Tb11.v5.0340	Tb927.4.3570	Tb05.5K5.70
Tb11.v5.0391	Tb927.7.2370	Tb11.v5.0659
Tb11.v5.0414	Tb927.8.6180	Tb927.11.6180
Tb11.v5.0501	Tb927.9.15110	Tb927.5.4420
Tb11.v5.0611	Tb927.9.7590	Tb927.7.1740
Tb11.v5.0683		Tb927.7.1750
Tb11.v5.0763		Tb927.9.11470
Tb11.v5.0877		Tb927.9.1810
Tb11.v5.1046		Tb927.10.5360
Tb927.10.1080		Tb927.10.5460
Tb927.10.11540		Tb927.7.5170
Tb927.10.14600		Tb927.8.1330
Tb927.10.14630		Tb11.v5.0851
Tb927.10.15120		Tb11.v5.0181
Tb927.10.2090		Tb11.v5.0182
Tb927.10.2100		Tb11.v5.0243
Tb927.10.3840		Tb11.v5.1060
Tb927.10.3930		Tb927.10.5330
Tb927.10.4110		Tb927.10.5610
Tb927.10.6090		Tb927.3.3310
Tb927.10.8270		Tb927.4.2720
Tb927.11.10790		Tb927.7.5000
Tb927.11.11230		Tb11.v5.0637

Tb927.11.12880		Tb927.10.7560
Tb927.11.13090		Tb07.11L3.90
Tb927.11.14000		Tb927.7.2140
Tb927.11.2050		Tb11.v5.0465
Tb927.4.1790		Tb927.10.15650
Tb927.4.3550		Tb927.10.13570
Tb927.6.4690		Tb927.1.1790
Tb927.7.1040		Tb927.10.1260
Tb927.8.740		Tb927.11.3890
Tb927.9.11380		Tb927.2.4740
		Tb927.4.3020
		Tb927.10.2580
		Tb927.2.6070
		Tb927.10.7470
		Tb927.1.1500
		Tb927.5.4320